Science & Technology Facilities Council

Technical Report
RAL-TR-2013-002

Monte-Carlo simulations for the development of TOSCA's guide at ISIS

J Fernandez Castanon

April 2013

RAL Library
STFC Rutherford Appleton Laboratory
R61
Harwell Oxford
Didcot
OX11 0QX

Tel: +44(0)1235 445384
Fax: +44(0)1235 446403
email: libraryral@stfc.ac.uk

Science and Technology Facilities Council reports are available online at: http://epubs.stfc.ac.uk

ISSN 1358- 6254

Monte-Carlo simulations for the development of TOSCA's guide at ISIS

Javier Fernández Castañón *

Summer 2012

ISIS Neutron and Muon Source

Science and Technology Facilities Council. Rutherford Appleton Laboratory.

Harwell Oxford, Didcot, OX11 0QX

United Kingdom

Abstract

McStas software package offers the possibility to determine accurate estimates for flux, resolution and optimization parameters with the aim to achieve the best guide for TOSCA instrument, sited at ISIS.

Different simulations are compared, defining new perspectives for instruments similar to TOSCA, pursuing optimize the resolution with the minimum costs.

Most of the instruments which have at their disposal a neutron guide have lengths greater than 50 or 60 m, as for example the instrument HRPD- ISIS TS1.

The astonishing gain obtained installing a neutrons guide, which has been developed attending the particular properties established by a pioneering world-wide instrument as TOSCA, justifies and stipulates the path what has to be followed in the future for instruments with similar characteristics, becoming TOSCA as a point of reference in Inelastic Neutron Scattering (INS) research.

*javixu5@hotmail.com UO204021@uniovi.es

Acknowledgments

I would like to thank **all the people who have helped me** during my work at ISIS.

My most sincere thanks to **Robert Bewley** for all the time spent teaching me during talks and for his first results used as point of reference for the develop of this report.

I would like to thank as well the collaboration of the engineers, **Simon Waller, Leigh Perrot** and **Peter Galsworthy**, for our profitable discussions.

Por supuesto a mis asturianos preferidos de todo el Laboratorio. El Concejo de Aller ha quedado bien representado. **Vicky**, thank you very much for your time hosting and helping me during the first days, here, at ISIS. For our conversations, for your sympathy and kindness, and for everything I have learned from you, more than you can imagine. Thanks for you too, **Félix**, to offering me this wonderful experience and for trust me since the *"first email sent to nobody"*.

And last but not least, thank you so so much **Timmy**. You wouldn't believe all I've learned from you these months, not only in scientific tasks but also for opening me new future prospects. Thank you for encouraging me both personally and professionally, and for supporting and advising me in every aspect of my work, sometimes leaving in the background your own labor issues.

A **Paula**, por estar siempre ahí.

Y, por último, quiero dedicar este trabajo **a mis padres** por haberme permitido llegar hasta aquí. ¡Gracias **mamá**!, en estos momentos tan difíciles, por tu fuerza y apoyo, sin los cuales nada de todo esto habría sido posible. A **Jaime**, a **Anina, Chema, Viole, Arias** y **Mª José**.

Thanks. Gracias.

Javi

Contents

Part I
Executive summary

At the moment there is increased competition in the area of molecular spectroscopy with neutrons. There are two new instruments that can study similar parts of the spectrum as TOSCA, namely: VISION, at the SNS, and LAGRANGE, at the ILL.

1 Background

The new SNS instrument VISION is being commissioned. VISION has set the bar very high. At the moment, extrapolating from the initial measurements in VISION [Private communication] the total flux at sample position is around 50 to 100 times the flux in TOSCA. This can be divided into, more neutrons due to the extra power of the SNS plus the fact the VISION has a neutron guide that effectively multiplies the number of neutrons at sample position. This, in conjunction with a larger effective detector area and higher resolution crystal analyzers, also makes VISION's instrumental resolution twice as the one of TOSCA at the elastic line.

In short, without a neutron guide TOSCA will be a second class instrument that will not be able to compete with VISION, and in it keeps its present configuration without a guide form it will be its demise.

2 What if TOSCA has a guide?

Taking into consideration all the simulations and installing a neutron guide to TOSCA like the one described below, will give us the gains shown in Table 1 and listed in Table 2 compared with the present instrument configuration.

TOSCA has, thanks to the new 10Hz chopper unique access to the elastic line and the inelastic region with a smooth and continuous resolution function ($\Delta\omega/\omega \sim 1.25\%$) in the 3-1000 meV range and ($\Delta\omega \sim 300\mu eV$) around the elastic line. In its present configuration VISION cannot access the elastic line regain and can only access the 5-1000 meV range.

It is clear that these gains will put TOSCA back in the map and make it competitive again. The guide, combined with the the development of the 10Hz chopper will make TOSCA untouchable in its capabilities worldwide, since there is no instrument, either already built, in commissioning or even planned that can access the dynamical range with the high resolution that TOSCA will have as consequence of these modifications.

McStas Name	$\mathbf{w_1}$=$\mathbf{h_1}$ **(m)**	$\mathbf{w_2}$=$\mathbf{h_2}$ **(m)**	**AT (m)**	**l (m)**	m	Area/m^2
guide_shutter	0.100	0.100	1.625	1.938	3	0.7752
guide_gap (*)	0.100	0.100	3.565	0.110	0	
guide1_1	0.100	0.092	3.695	1.500	3	0.576
guide1_2	0.092	0.088	5.200	0.845	3	0.3042
guide2_1	0.088	0.080	6.0405	1.5000	3	0.504
guide2_2	0.080	0.073	7.5410	1.4540	3	0.445
guide_vac_val	0.073	0.073	9.0270	0.0380	0	
guide3	0.073	0.071	9.0655	0.3465	3	0.099
guide4 (Chopper)	0.071	0.071	9.4120	0.0870	0	
guide5_1	0.071	0.063	9.5045	1.5000	4	0.402
guide5_2	0.063	0.055	11.0050	1.5000	4	0.354
guide5_3	0.055	0.047	12.5055	1.5000	5	0.306
guide5_4	0.047	0.040	14.0060	1.5000	5	0.261
guide5_5	0.040	0.038	15.5065	0.2585	6	0.403
guide6_1	0.038	0.035	15.7655	0.6000	6	0.088

Table 1: TOSCA's guide setup.

Energy at sample (meV)	**Gain**
10	39.5
20	24.3
50	12.2
100	7.4
150	5.1
200	3.9
250	3.3
300	2.7
350	2.5
400	2.4
566	1.9

Table 2: Gain achieved with TOSCA's guide.

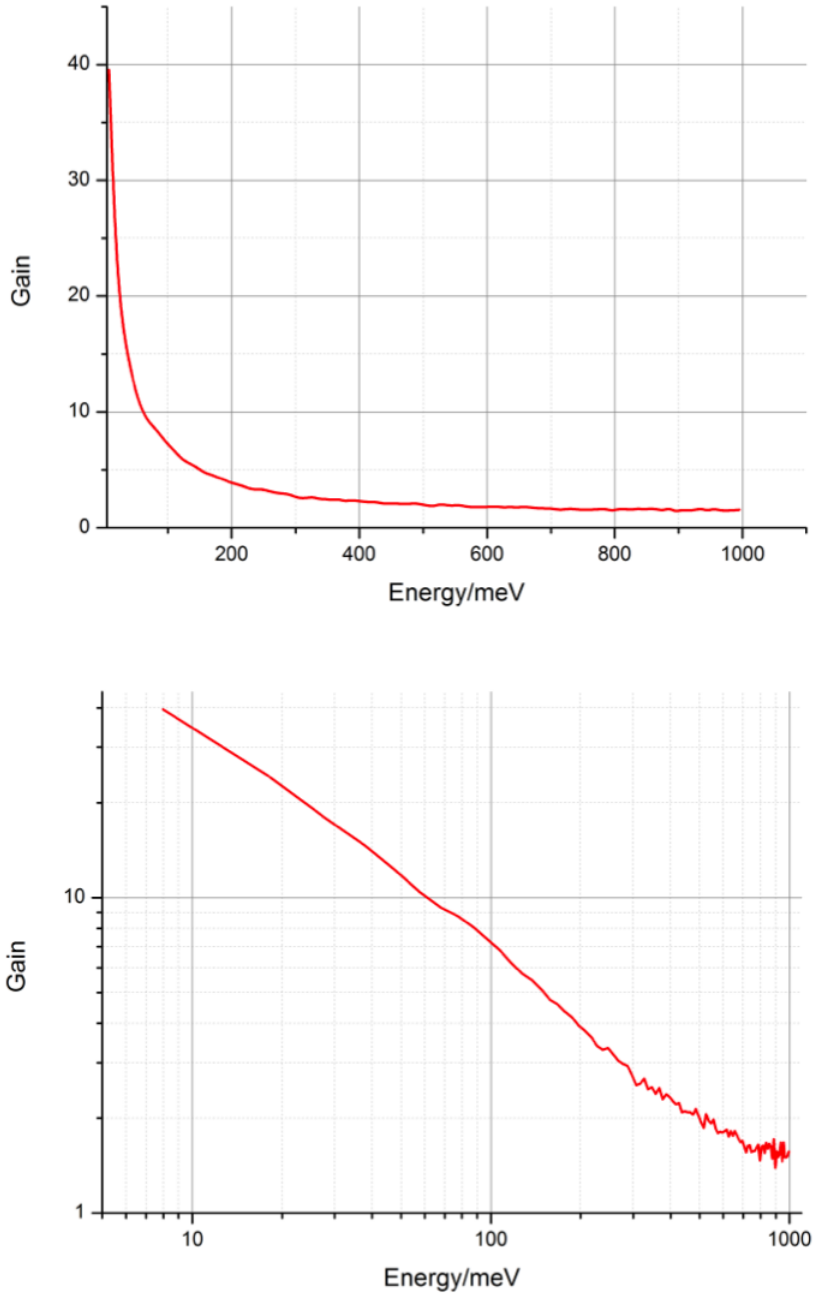

Figure 1: Gain achieved with TOSCA simulated guide between 0 and 1000 meV. Top, linear scales, bottom in logarithmic plot.

Part II
The modeling of the TOSCA guide

3 Introduction

3.1 Why neutrons?

Neutron sources are much less intense than X-ray sources, and therefore neutron scattering is an expensive and time consuming process, which means that neutron scattering is usually only used when other techniques cannot be adequately applied. However, neutrons have a number of advantages over X-rays which enable them to probe aspects of samples which are impossible to do with X-rays[1]:

- Compared to X-rays, neutrons can have a both low energy and wavelength, with a 20 meV neutron having a wavelength of about 2 Å. This enables neutron scattering to be used simultaneously for studying both the structure and excitations of materials.

- Neutrons can be effectively used to study light elements, such as hydrogen which is almost invisible to X-rays, as the neutron can scatter off the nucleus of an atom, not just the electron cloud. Additionally, this means that neutrons can distinguish between different isotopes of the same element.

- Neutrons can penetrate far into most materials, enabling the probing of a sample beyond its surface.

- Another advantage of the penetrative ability of neutrons is that samples can be enclosed in containers, thus allowing for the study of materials under extremes of temperature, pressure, external magnetic fields, etc.

- While the neutron is an uncharged particle, it is composed of positively and negatively charged quarks which forms a spin of $s = \frac{1}{2}$. This means that neutrons will react to magnetic fields sufficiently to allow neutron scattering to probe the magnetic structure of materials. A number of methods have been used to generate sufficiently strong neutron sources, but all current facilities are either fission reactors or spallation sources, so we will consider only these two methods.

The most powerful research reactor is the Institut Laue Langevin (ILL, Grenoble, France). The production of neutrons at a spallation involves high energy protons hitting a heavy metal target and as a by product of the induced nuclear reactions, neutrons are produced. The world has three major spallation neutron sources, ISIS the most productive spallation neutron source, SNS in Oak Ridge Tennessee, USA and J-SNS part of JPARC in Japan are the most powerful spallation neutron sources; the European Spallation Source (ESS) in Lund, Sweden is at design stage.

Inelastic Neutron Scattering is a very powerful tool to study hydrogen containing materials. With the development of neutron spallation sources, and the use of epithermal neutrons, incoherent inelastic neutron scattering can measure

the vibrational spectra of materials on the whole range of vibrational motions (0-1000 meV) effectively opening up the field of neutron spectroscopy.

3.2 Focusing the future. Neutron guides and Mirrors

Neutrons as particle waves follow the same law for the total reflection as light waves. Neutrons can move freely in vacuum. To construct a neutron mirror or neutron guide the first question to solve was to find a medium for neutrons, which is optically "thinner" than vacuum. Scientists found such a medium, which is a multi-layer system containing layers with alternating scattering characteristics (scattering length) and decreasing thickness.

Nowadays one can produce neutron mirrors made of several hundred double layers of nickel-titan. The limiting angle for total reflection of a neutron mirror is much smaller than for light in the optical glass fiber; it also depends on the neutron wavelength's. A rough formula for the limiting angle for neutrons is 1° times the wavelength of neutrons in nanometer, which results for the wavelength of 0.5 nm to approximately 0.5°. This small angular range for the total reflection reduces the efficiency in comparison to an optical glass fiber, but it still allows transporting neutrons to a remarkable distance up to 10 - 50 meter. This aspect has to be considered attending to TOSCA's length, from the moderator to the sample, 17m.

The transmission of neutrons is improved by using so-called super-mirrors, with limiting angles larger by factors 2 - 3 as compared to normal neutron mirrors. Super-mirrors are using for example layer systems with alternating layers of pure isotopes ^{58}Ni and ^{62}Ni, which differ even more in their neutron scattering properties (scattering length). As such layer systems are rather expensive (material costs) there are limits of possible applications to just a few cases.

The path of a neutron may be modified within certain limits by varying the reflection conditions on the guide walls. The range for reflection is, however, relatively narrow, specifically an incident angle of approx. 0.1°-1°, depending upon the energy of the neutron. It is nevertheless possible to deflect or guide the neutrons so as to improve experimental conditions, the aimed objectives are:

-to achieve high neutron intensity at the experiment with low background radiation,

-to split beams in order to supply several instruments,

-to ensure optimal utilization of the neutron source,

-to enable optimal utilization of the available space,

-if required, to polarize neutrons.

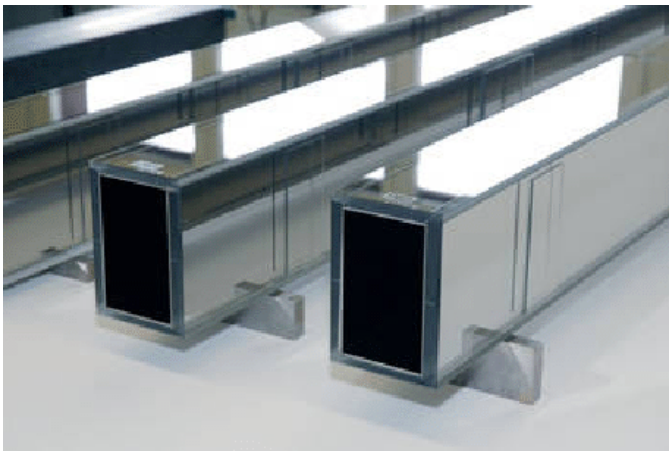

Figure 2: Straight neutron guides from SwissNeutronics.

In addition to conventional straight neutron guides, a modern neutron guide installation also contains special systems such as neutron guide switches, curved and focussing sections as well as novel coatings known as neutron super-mirrors. Here is where TOSCA makes the difference with the other instruments.

This effect is achieved if the length of the curved section is sufficient to ensure that no particles can reach the measuring position by a direct path, i.e. without reflection. Due to its high energy, the background radiation cannot be reflected and thus exits from the guide at the point of contact, unlike the majority of the cold and thermal neutrons. Focussing guides increase the neutron flux density at the sample. Such guide elements taper in one or two dimensions. The spatial compression is accompanied by an increase in the divergence of the neutron beam, which can be tolerated in many instrument and experiments. A similar situation applies to neutron guides with the above-mentioned super-mirror coating, in which a multilayer coating of variable thickness increases the range of reflexion angles. This multiplies the incident angle at which the neutrons are still reflected, so meaning that more neutrons are gathered and conveyed to the experiment. The characteristics of the super-mirror are advantageous in particular for focussing and curved guides. In focussing guides, the reduction in cross-section may be greater, which also increases the degree of compression of the neutron beam.

3.3 TOSCA's environment and basic INS theory

TOSCA is an indirect geometry time-of-flight spectrometer at the ISIS pulsed spallation neutron source at the Rutherford Appleton Laboratory [2]. TOSCA has replaced the previous spectrometers TFXA and TOSCA-1, however, it retains the advantages of the earlier instruments (ease of operation and reliability) but simultaneously offers improved sensitivity and resolution.

TOSCA is a collaborative project between the *Consiglio Nationale Recherche*

(CNR) of Italy, the *Department of Physics at the University of Kent at Canterbury* (UK) and *ISIS*. (For a detailed list of the participants see the TOSCA website http://www.isis.rl.ac.uk/molecularspectroscopy/tosca/ and the CNR website: http://www.ifac.cnr.it/tosca/tosca-main.htm).

TOSCA was installed in two phases: *Phase 1* was completed in May 1998 and consisted of the backscattering spectrometer at 12 m, *Phase 2* added detectors in forward scattering and moved the spectrometer to 17.0 m. This was completed in September 2000. The move to 17 m from 12 m has resulted in a large improvement in resolution.

It is optimal in the energy range 0 - 4000cm^{-1} (0 - 500 meV) with the best results below 2,000 cm^{-1}, (250 meV). To suppress the &gamma-flash and fast neutron background a Nimonic chopper is installed at 9.5 m. This has a tailcutter (a sheet of B_4C) on the leading edge to remove low energy neutrons that would otherwise result in frame overlap.

The source of neutrons on TOSCA is the white beam from the water moderator. The time-of-flight technique is used for energy analysis of the scattered neutrons. A small fraction of the incident neutrons are inelastically scattered by the sample; those that are backscattered through an angle of 45°or 135° impinge on a graphite crystal.

Bragg's law states:

$$\lambda = 2\ \mathrm{d}\ \sin\theta \tag{1}$$

where d (Å) is the interplanar distance in the crystal, λ (Å) is the wavelength of the scattered neutron and ϑ is the angle of incidence on the crystal.

From equation (1) , since both d and θ are constant only one wavelenght (and its higher orders, $\lambda/2$, $\lambda/3$ etc...) will be Bragg scattered by the crystal, the remainder will pass through the graphite crystal to be absorbed by the shileding. The neutrons at multiples of the fundamental wavelenght are scattered by the beryllium filter which acts as a longpass filter and the remaining neutrons are then detected by the ^{3}He filled detector tubes. The net effect of the combination of the graphite crystal and beryllium filter is to act as a narrow bandpass filter.

The energy transferred to the sample, E_{trans}, is:

$$E_{trans} = E_i - E_f \tag{2}$$

where E_i and E_f are the incident and final energies respectively. The kinetic energy, E, of a neutron is given by:

$$E = {}^{mv^2}/_2 \tag{3}$$

where m is the mass of the neutrons and v is its velocity. Rearranging (3) gives:

$$v = \sqrt{\frac{2E}{m}} \tag{4}$$

and since

$$travel\,time = distance/velocity \tag{5}$$

It follows that the time of arrival at the detector, T, is the sum of the time from the moderator to the sample, t_i , and the time around the analyzer, t_f, thus:

$$T = t_i + t_f = \frac{L}{v_i} + \frac{l}{v_f} = {}^{L}/\sqrt{\tfrac{2E_i}{m}} + {}^{l}/\sqrt{\tfrac{2E_f}{m}} \tag{6}$$

Now since the final energy, E_f,the distance round the analyzer system, l, and the length of the flight path from the moderator to the sample, L are all known, it follows that the time of arrival at the detector uniquely defines the incident energy, E_i and hence the energy transfer at the sample, E_{trans}. Thus it is a simple matter to convert from time-of-flight to energy. The result is a spectrometer with no moving parts than can record spectra from 0 to 8000 cm^{-1}. The resolution of the spectrometer is determined by number of factors but for practical purposes can be taken to be 1.25% of the energy transfer.

The intensity of the molecular vibrational transition is proportional to:

$$I_i \propto Q^2 U_i^2 exp\left(-Q^2 U_{Total}^2\right)\sigma \tag{7}$$

Since neutrons have a mass approximately equal to that of the hydrogen atom, an inelastic collision results in a significant transfer of momentum, Q($Å^{-1}$), as well as energy, to the molecule. On TOSCA the design is such that there is approximately one value of Q for each energy ($Q^2 \approx {}^{E_{trans}}/_{16}$). (Other instruments at the ISIS Facility and the ILL allow both the energy and the momentum transfer to be varied, but they constitute a different story). U_i is the amplitude of vibration of the atoms undergoing the particular mode. The exponential term in equation (7) is known as the Debye-Waller factor, U_{Total} is the mean square displacement of the molecule and its magnitude is in part determined by the thermal motion of the molecule. This can be reduced by cooling the sample and so spectra are typically recorded below 50K.

σ is the inelastic neutron scattering cross-section of all the atoms involved in the mode. The scattering cross-sections are a characteristic of each element and do not depend on the chemical environment. The cross-section for hydrogen is ~80 barns while that for virtually all other elements is less than 5 barns. This means that modes than involve significant hydrogen displacement will dominate the spectrum. This dependence on the cross-section is why the INS spectrum is different from infrared and Raman spectroscopies. There, the intensity derives from changes in the electronic properties of the molecule that occur as the vibration is executed, (the dipole moment and the polarisability for infrared and Raman spectroscopy respectively).

A consequence of the indirect geometry is that for energy transfers >100 cm^{-1} the momentum transfer vector is essentially parallel to the incident beam. The significance is that for an INS transition to be observable there must be a component of motion parallel to the momentum transfer vector. This means

that with oriented samples (such as single crystals or aligned polymers) measurements directly analogous to optical polarization experiments carried out.

In addition to the inelastic detectors there are also two ^{3}He filled detector tubes either side of the incident beam (scattering angle $\approx 179^{o}$). These are for elastically scattered neutrons and enable high resolution, Δ d/d $\approx 3\times10^{-3}$, diffraction patterns to be recorded simultaneously with the inelastic spectrum. It is planned to install two further banks of diffraction detectors at 45 and 135^{o}. The purpose of the detectors is to provide a check on the crystal phase of the material and to monitor phase changes as an experimental variable is changed *e.g. t*emperature and pressure. There is also a low efficiency scintillation detector (the monitor) in the main beam just before the cryostat vacuum tank. This measures the incident flux distribution as a function of time and is used to normalise the spectra.

For further information reading *TOSCA User Manual* [3] is recommended.

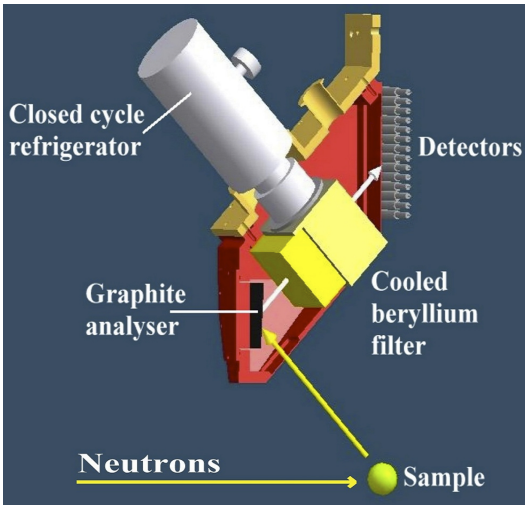

Figure 3: A section through one of the analyzer modules of TOSCA.

The TOSCA spectrometer undergone a series of improvements and it is at the present the best instrument of its type in world. The series of modifications that have enhanced TOSCA are: the modification of the Be filters (2005), the new frame overlap chopper (2010) and the modified cryostat (2011). Overall the first modification reduced the background by a factor of 50-100; the chopper allows the access to the elastic line while TS2 is operating, the new cryostat improves the cooling time dramatically (10 minutes from room temperature using LHe). At the moment TOSCA is limited in the science by the available flux. The only avenue for improvement is to insert a neutron guide to increase the amount of neutrons at the sample position. There are two instruments that will compete with TOSCA in the near future, LAGRANGE at the ILL and VISION at the SNS. If TOSCA wants to remain competitive the flux has to be

increased.

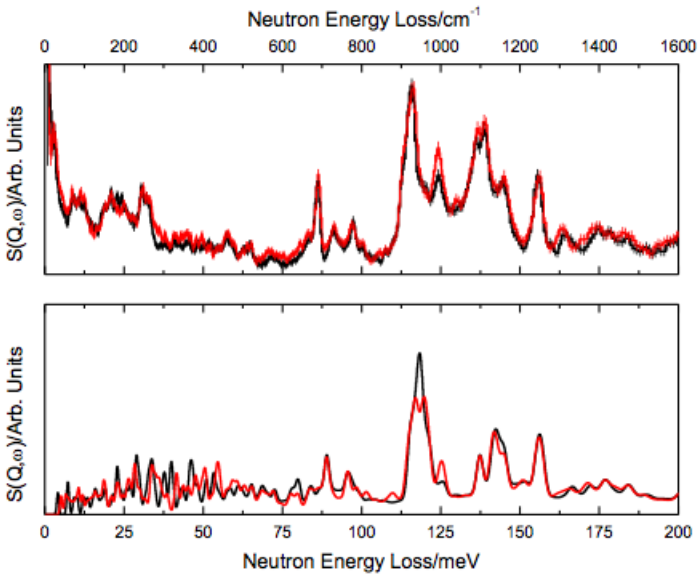

Figure 4: Neutron Energy Loss up: cm^{-1} down: meV

As it is shown in Section 2 the gains in flux for TOSCA are close to a 40-45 factor for low energies, that will open new fields of science, a recent example has been the study of CO_2 adsorption in Metal Organic Frameworks by Martin Schröeder and Sihai Yang from Nottingham University[4]. The induced changes in the vibrational modes due to the adsorption of CO_2 could be observed, but the time required for the measurement was 9 days. However not only this, but also, most important point for TOSCA is the gain, more than 5 times compared against the actual situation of TOSCA, at higher energies (150 meV).

4 Results and Discussion

4.1 Guide Geometry

Many different guides were considered and simulated , using the *Neutron Ray-Trace Simulation package McStas[5]*, trying to get the maximum flux at the sample with the lowest economical cost.

4.1.1 Guide Configuration

The component **guide,** used in McStas simulations, models a guide tube consisting of four flat mirrors. The guide is centered on the z axis with rectangular

entrance and exit openings parallel to the x-y plane. The entrance has the dimesions (w_1, h_1) and placed at z=0. The exit of dimensions (w_2, h_2) and is places at z=l where l is the guide length. See figure 5. The reflecting properties are given by the values of R_0, m, Q_c, W, and α detailed in **Part II** and Table 21 on page 51.

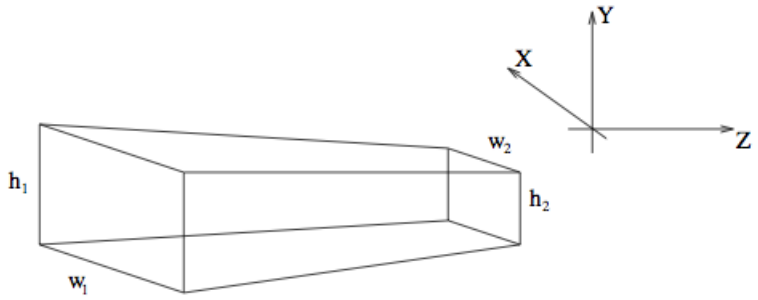

Figure 5: Geometry used for the guide component.

The parameters which provide these conditions, and get us a minimum in the divergence, are detailed next.

The distance between the center of the moderator and the sample is 17.0 m, which compared with the distances existing in other instruments, such as HRPD-ISIS TS1, with an elliptical guide 90 m long, can be classified as a short "*potential*" guide. Not only that, but also the wish of increase the gain in the range of high energies forced us to consider a *simple design* for the guide . The usefulness of a ballistic guide in TOSCA is invalidated by the short effective distances have the energetic neutrons to be reflected by the super-mirrors that are covering the guide.

Therefore the main options to take into account are a straight or a tapered guide, or, why not, a union as combination of both of these cases.

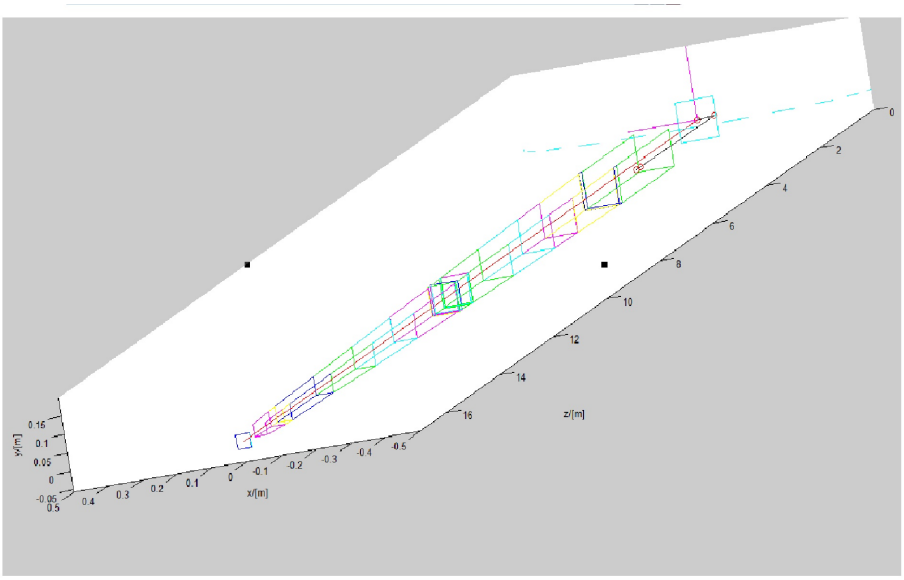

Figure 6: TOSCA final design. First green section, shutter guide, corresponds to a straight shape, followed by a tapering guide with 0.10 m size at the start and 0.035 m at the exit.

4.1.2 Source and Moderator

The center of the moderator is located at the point established as "Origin", and relative to this absolute position (0,0,0) are defined all the distances and components of the guide.

A H_2O moderator at 300 K poisoned with Gd at 2.5 cm is installed in TOSCA. This moderator provides a short time pulse with an energy range appropriate for the design of this spectrometer.

The source is defined with an energy range between 0 and 1000 meV and the distance from the source to the focusing rectangle is 1.625 m (all the distances and components are listed in the Appendix 6.2 on page 47). According to the instrument properties both width and height of focusing rectangle are 11 cm, as well as the moderator vertical and horizontal sizes.

Further, up to the shutter position, Void Vessel Windows and the Collimation Ray Layout are located. The shutter starts at 1.625m from the origin. Defining the guide there are three parameters that are constant through all the guide, regardless its shape or size, listed in Table 3:

McStas Parameter	Value
alphax (Å)	4.38
alphay (Å)	4.38
W ($Å^{-1}$)	$3e^{-3}$

Table 3: Fixed parameters for TOSCA's guide simulation. See Table 21 on page 51 for further details.

Note that the values used for theses parameters are the default values used by McStas to simulate a typical neutron guide.

4.1.3 Shutter and Monolith (insert)

There are three major areas where the guides have to be positioned, the shutter, monolith (insert) and the rest of the primary spectrometer. The guide in the **shutter**, is probably an expesive proposition, the **shutter** is too hot (radioactive) to be handled and a new shutter will be required in order to have a guide inside it. In the case of the **shutter** guide the first task is to systematically analyze the cross section at the guide entry. The reason is that an aperture greater than the aperture of the moderator will result in a loss of the total number of neutrons that will reach the sample, due to the number of neutrons with an incident angle below the critical angle is going to be reduced. Figure 7 shows the best size for the height and width at the guide entry.

As it shown, the highest gain is given for an amplitude of 0.10 m, that is 2 cm less than the size of the moderator. The orange line shows the reference of 0.12m (first option taken into account in the original simulations) relative to which all comparisons have been done, before noticing that the critical angle existing with this initial amplitude was not reflecting a percentage of the initial neutrons.

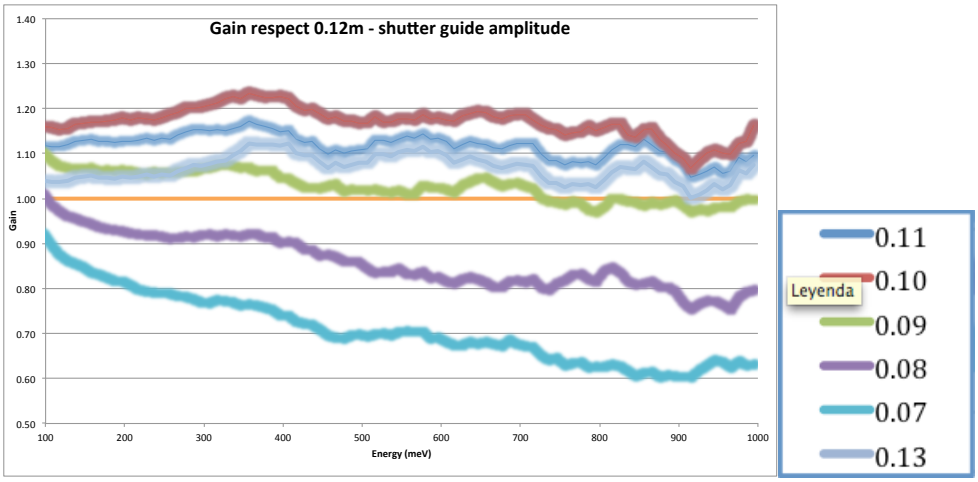

Figure 7: Gain against Energy at the sample (meV), compare with the energy at sample for 0.12 x 0.12 m cross section at shutter guide entry.

According to that an amplitude of 0.10 x 0.10 m was selected. To decide if this guide should be tapered or straight both simulations were done. The configuration selected for this purpose was a tapering guide with constant slope after the shutter guide and reshaping the guide in the shutter to be straigth or tapered. Results are shown in Figure 8 in two graphs that only differ in the energy scale, as a zoom until 300 meV.

At energies greater than 200 meV the benefits can be neglected, the mean physical reason is that most energetic neutrons will reach the sample without reflections in the mirrors, ergo the guide does not exist for them, and because of that the geometry of the guide is irrelevant in this case.

In the scale 0-300 meV (top plot in Figure 8) small differences can be observed. The variations are detailed in Table 4, presented below.

The straight shutter guide has been chosen as the best option since the gain values, compared with tapered shutter guide are very similar and for engineering requirements the simplicity of a straight guide is preferred in a delicate area such as the shutter. As it displayed, it is recommended include the guide in the shutter, since the loss in the factor guide is important in the 5-150 meV range if the guide is removed.

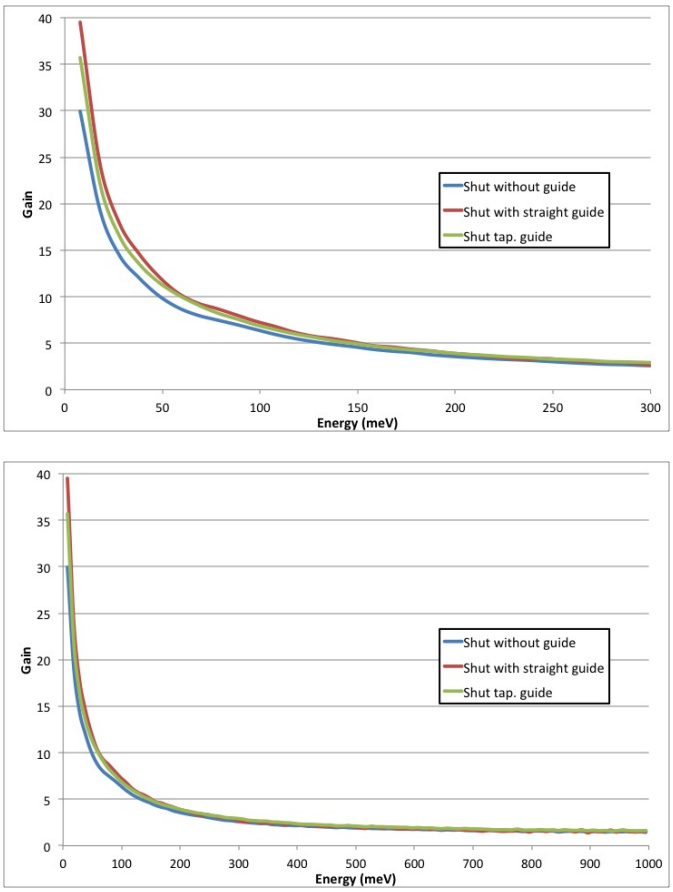

Figure 8: Gain against Energy at the sample (meV) for different guides in the shutter, with respect to current situation of TOSCA with different energy scales.

Energy at sample (meV)	Gain Shutter Guide		
	Straight	Tapering	Without Guide
10	39.5	35.7	30.0
20	24.3	22.2	19.4
50	12.2	11.6	10.1
100	7.4	7.0	6.5
150	5.1	5.0	4.6
200	3.9	4.0	3.6
250	3.3	3.3	3.1
300	2.7	2.9	2.6
350	2.5	2.7	2.4
400	2.4	2.4	2.2
566	1.9	2.0	1.8

Table 4: Gains for different shutter guides.

Between the shutter and the monolith there is a gap of 0.110 m length, that for technical reasons is not possible to avoid and can be understood as a completely absorbing section for neutrons.

Then, in the **monolith**, that starts at 3.695 m from the moderator center, has been thoughtfully considered a tapering guide of 2.35 m length , with 0.10 m width and height at the guide entry and 0.088 m at the guide exit.

The benefits of installing a tapering section until the exit of the monolith instead a straight guide are detailed in Figure 9 and Table 5. Simulation has been done considering a straight guide in the shutter, a tapering guide with constant slope after the monolith and until the end of the guide, simply changing the guide's shape in the monolith.

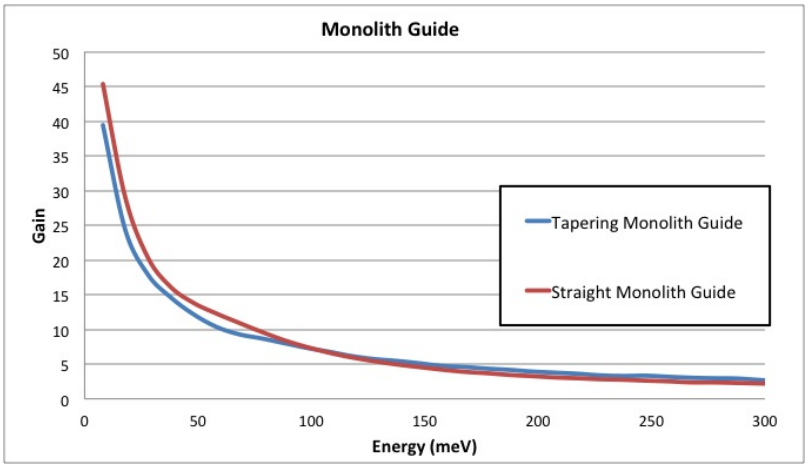

Figure 9: Gain for Straight and Tapering Monolith Guides.

Energy at sample (meV)	Gain Monolith Guide	
	Tapering	Straight
10	39.5	45.3
20	24.3	29.0
50	12.2	13.9
100	7.4	7.5
150	5.1	4.6
200	3.9	3.3
250	3.3	2.6
300	2.7	2.2
350	2.5	2.0
400	2.4	1.8
566	1.9	1.5

Table 5: Gains for Straight and Tapering Monolith Guides.

The gain with a straight guide in the monolith is greater than with a tapering one but just up to 120 meV. Gains as 7.4 at 100 meV or 5.1 at 150 meV suggest that a ***straight*** guide in the ***shutter*** and a ***tapering*** shape in ***monolith*** display the best results.

The final guide setup in the shutter and the monolith is detailed in Table 6.

McStas Name	w_1=h_1 (m)	w_2=h_2 (m)	AT (m)	l (m)
guide_shutter	0.10	0.100	1.625	1.938
guide_gap (*)	0.10	0.100	3.565	0.110
guide1_1	0.10	0.092	3.695	1.500
guide1_2	0.092	0.088	5.200	0.845

Table 6: Shutter and Monolith guide. Setup. See Table 21 on page 51 for further details.

(*) guide_gap presents no guide. See 4.1.3 on the preceding page.

4.1.4 Tapering Guide

In this position, at the end of the monolith, there are still more than 10 m of guide that has to be specified. It is essential convey the biggest amount of neutrons to the sample but only if it does not imply a huge divergence. The guide has to be designed following this aim, it should allows *good* neutrons remain inside the guide while neutrons which only provoke divergence are thrown out.

Different options were considered for simulating the guide, however is required a guide which focalized the beam to the sample, which has a section of 3.5 cm. As it is shown in Figure 12 different geometries of the guide (e.g.: elliptic behavior) give us higher gains at energies lower than 150 meV, but it decreases at greater energies. The case of **straight shape through all the guide** is considered as well, see the gain plotted in Figure 10. The plot is for an unrealistic guide of 12×12 straight guide (the sample size is 4×4).

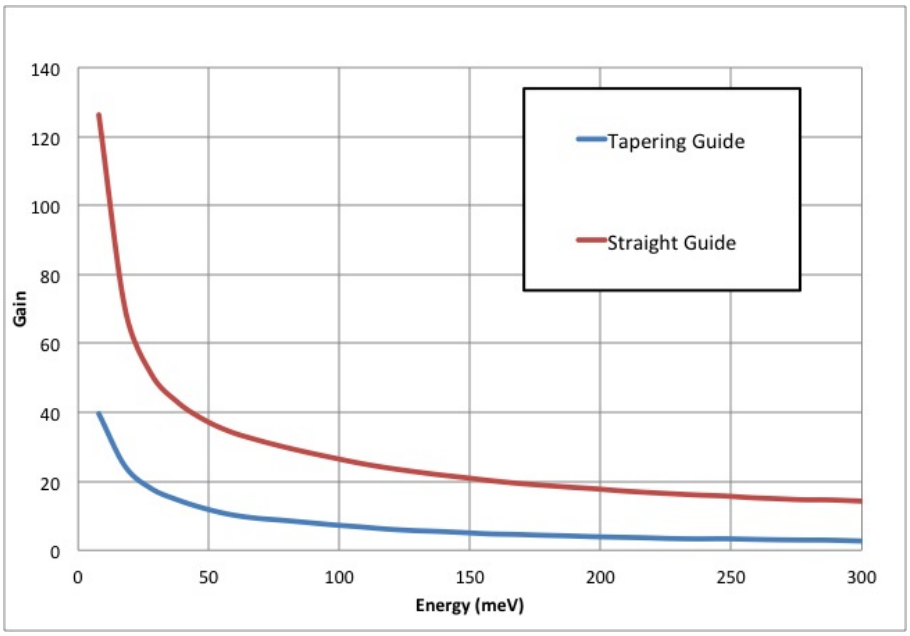

Figure 10: Gain obtained between 0 and 300 meV. Straight guide compared with Tapering guide between 6.04 m from the moderator until the sample.

Degrees (+/-)	Tapering Guide (10^5)	Straight Guide (10^5)
0	8.2	72.3
0.3	6.6	65.1
0.5	4.8	30.2
0.7	2.2	11.2
0.9	1.1	7.0
1.1	0.8	—

Table 7: Straight and Tapering guides. Divergence.

The huge defocusing at the exit of the guide, nearly the sample position, implies that the flux can not be maximized without a huge divergence correlated, see Table 7. In a straight guide the reflection angle is conserved and because of that the critical angle condition is checked in all the rebounds, allowing that all the neutrons achieve the sample and the flux becomes greater. That's not necessarily happens in a tapering guide where the angle after each reflection is increased, and can occurs that at certain position the neutrons do not have an angle of incidence below the critical angle anymore and exit the guide.

Regarding the elliptical guide, the differences with respect to the tapering shape can be ignored, within error bars. This means, according to this result, that there are not apparent reasons for selecting an elliptical guide, which im-

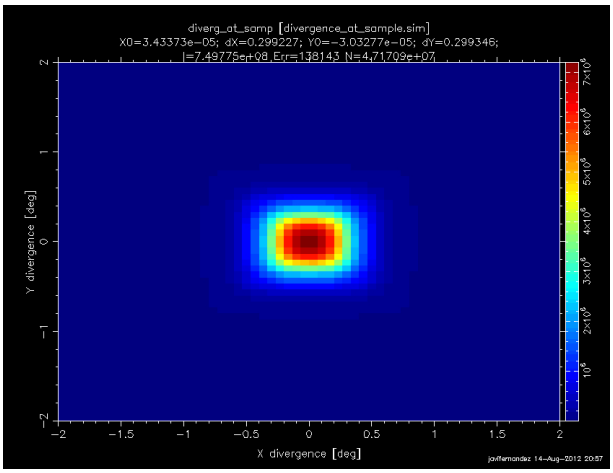

(a) Straight Guide

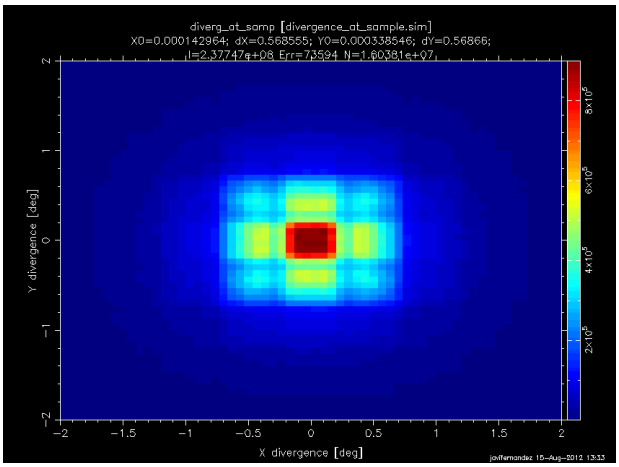

(b) Tapering Guide

Figure 11: Divergence

plies a complex design, composed of 30-40 straight guide sections, arranged to form an elliptic shape and at a increased cost of 20%. See Appendix 4.4 on page 33. Furthermore, considering the motivation for using an elliptical guide is to guide the neutrons to the sample precisely after one reflection increasing the intensity transmitted to the target. Liouville's theorem dictates that any gain in intensity on target must be offset by an increase in divergence. Thus for instruments which are very sensitive for divergence in both the vertical and horizontal directions, an elliptical guide geometry will likely be useless. As it has been studied in an ESS research, plying a 100 m guide, elliptical shapes are highly beneficial in large guides[6].

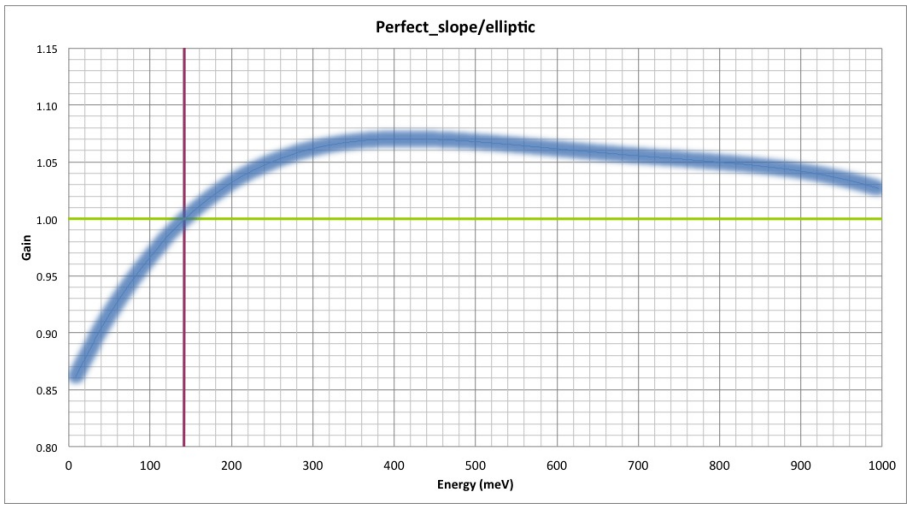

Figure 12: Ratio between Tapering Guide (constant slope) and Elliptic Guide.

In Figure 13 are plotted the graphs corresponding to the divergence and the intensity at the sample for elliptic and tapered guides for TOSCA.

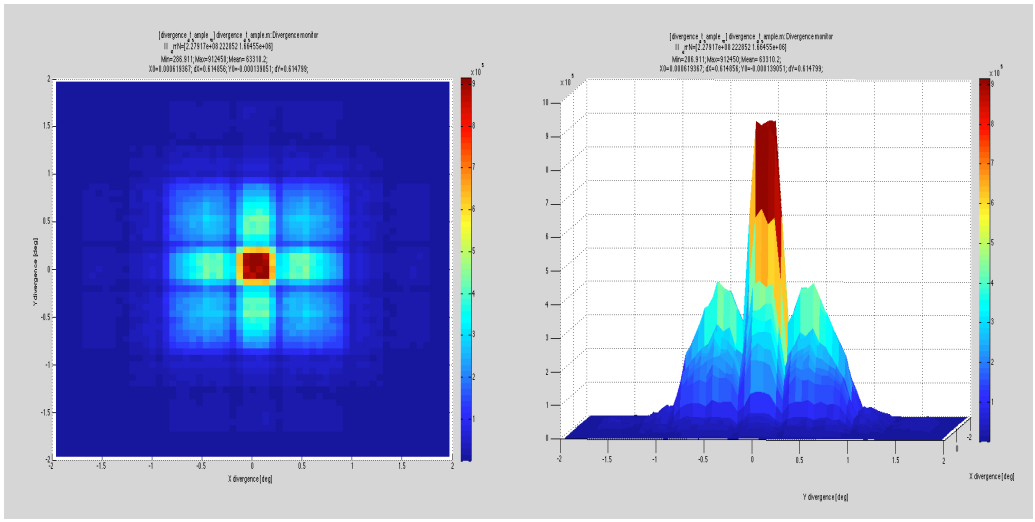

Figure 13: Divergence at the sample. Elliptical Guide Divergence. Left: 2D Right: 3D.

The remarkable divergence for the tapering guide appears up to 0.6 degrees while in the elliptical case is extended until 1.0 degrees. The peaks are $8.2{\cdot}10^5$ for tapering guide and $9.1{\cdot}10^5$ for the elliptical design. The divergence and the cost presented by the elliptical shape are not offset by the gain in TOSCA's

guide.

Degrees (+/-)	Tapering Guide (10^5)	Elliptical Guide (10^5)
0	8.2	9.1
0.3	6.6	7.2
0.5	4.8	5.4
0.7	2.2	3.9
0.9	1.1	2.8
1.1	0.8	1.4

Table 8: Divergence for Tapering and Elliptical guides.

Due to the symmetry through all the guide, square cross-sections, there are not privileged directions and as a consequence all the results present a perfect symmetry regarding the central position.

It was confirmed how an elliptical shape can modify the flux at the sample.

The gain values obtained simulating the tapering guide are detailed in Table 9.

Energy at sample (meV)	Gain
10	39.5
20	24.3
50	12.2
100	**7.4**
150	5.1
200	**3.9**
250	3.3
300	2.7
350	2.5
400	2.4
566	1.9

Table 9: Gain with tapering shape.

Tapering guide setup Depending on the energy range of interest, where maximize the flux, the slope of the tapering guide can be modified. More inclined mirrors placed at the exit of the gain give greater gain at low energies. Constant slopes through all the guide moderate this gains and compensate less gain at low energies with more gain at higher. The setups for the guide are sorted in Table 10.

McStas Name	AT (m)	l (m)	$w_1 = h_1$ (m)	$w_2 = h_2$ (m)
guide2_1	6.0405	1.5000	0.088	0.080
guide2_2	7.5410	1.4540	0.080	0.073
guide_vac_val	9.0270	0.0380	0.073	0.073
guide3	9.0655	0.3465	0.073	0.071
guide4 (Chopper)	9.4120	0.0870	0.071	0.071
guide5_1	9.5045	1.5000	0.071	0.063
guide5_2	11.0050	1.5000	0.063	0.055
guide5_3	12.5055	1.5000	0.055	0.047
guide5_4	14.0060	1.5000	0.047	0.040
guide5_5	15.5065	0.2585	0.040	0.038
guide6_1	15.7655	0.6000	0.038	0.035

Table 10: Tapering guide. Setup. See Table 21 on page 51 for further details.

The tapering guide is extended up to 16.36 m from the moderator what implies that **ends 0.63 m before the sample position**. At this point is essential to emphasize that the guide has to finish as close as possible to the instrument aiming obtain the greatest flux. Twenty simulations were made with the primitive design of the guide that gives less gain but allows compare the results as well, reducing the guide from 16.36 m (exit B) to 15.77 m (exit A), relative to the moderator. In this second case the exit of the guide is located 1.23 m before the sample. Figure 14 shows two gain branches perfectly differentiate which indicate the extremal necessity of extend the guide up to 0.63 m to the sample.

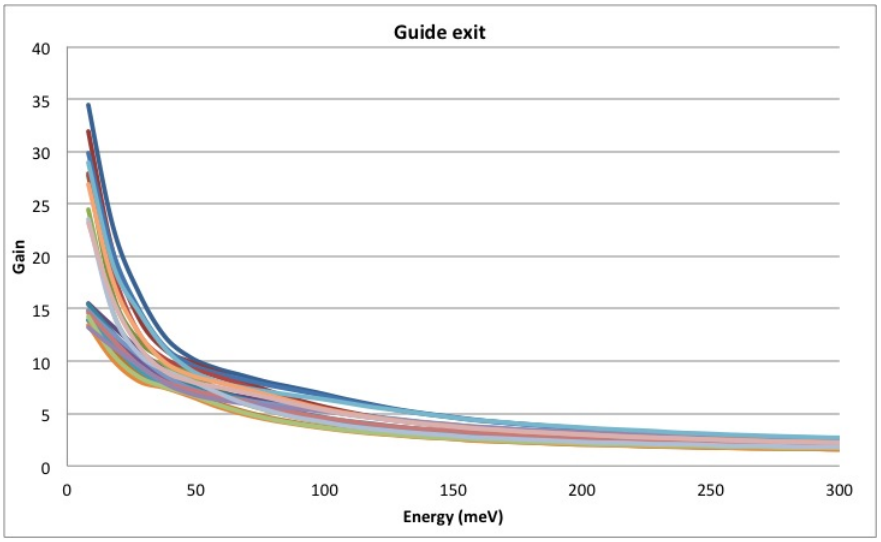

Figure 14: End of the guide. Top branch represents exit B - 16.36 m from mod. - while bottom branch represents exit A - 15.77 m from mod. It can be seen that for all combinations there is a loss of intensity if the guide is finished at 15.77m, so extending the guide after the diffraction detectors and before the conection between the spectrometer and the vacuum system.

Afterwards, the benefits of installing a **snout** until 0.28 m before the sample will be studied in Section 4.3 on page 31. Only the Vacuum Valve and the Chopper, which are assumed in the same way that gaps, represent straight sections, where there is not guide.

In addition, currently, between guide5_5 and guide6_1 is where the monitors and detectors are placed in TOSCA. The results presented previously were simulated taking into consideration a new design, more reasonable, in which the **monitors** allow the existence of the guide into and out of them.

Figure 15 and Table 11 display the comparison among these possibilities.

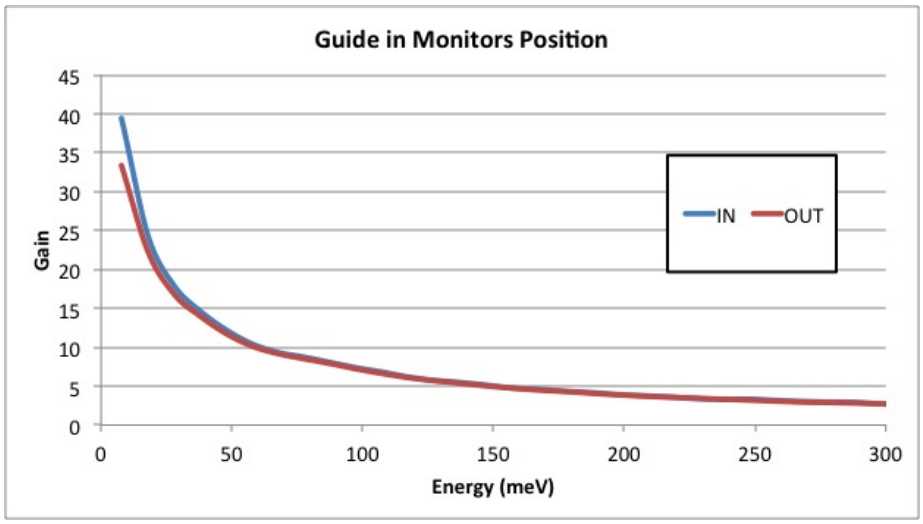

Figure 15: Gain in 0-300 meV energy range. Guide in/out monitors.

Energy at sample (meV)	Gain	
	Guide IN	Guide OUT
10	39.5	33.3
20	24.3	22.3
50	12.2	11.7
100	7.4	7.2
150	5.1	5.0
200	3.9	3.9
250	3.3	3.2
300	2.7	2.7
350	2.5	2.5
400	2.4	2.2
566	1.9	1.8

Table 11: Guide in/out monitors.

The differences are not so important, anyway, so when modifying TOSCA introducing the guide where the monitors are placed will improve the number of neutrons at sample position slightly.

4.2 Chopper Placement

The original Nimonic chopper on TOSCA has two purposes; it removes the γ-flash (γ-rays and suppress the prompt pulse of fast neutrons produced when the

proton beam strikes the target) which only contribute to background. There is a piece of B_4C on the leading edge of the chopper that removes slow neutrons from the neutron pulse preventing frame overlap. The chopper is phased to remove as many high energy neutrons as possible. The rotation rate should be 50 Hz and is phased to block the beam line when this background radiation is produced. The maximum transmitted energy depends on the blade width and radius, rotation speed, and position along the beam line. Probably after the installation of the guide the chopper will be modified installing a double plate chopper rotating in oposite directions. If an experimente requires a higher incident energy, would be interesant if the chopper was able to rotate at twice the source frequency to pass neutrons of higher energies.

All the results displayed before were made considering the chopper, 0.087 m length, located at **9.4 m from the moderator**. However TOSCA allows the chance of change this location to another one situated at 8.8 m, or even closer to the moderator, at 8.2 m. Theses changes suppose relative positions of **-0.6 m** and **-1.2 m** relative to the original position of the chopper.

Desiring obtain a comparison between all the possibilities, the simulations were made considering elementary guides that preserves the geometry, only changing the chopper position. However is useless compare this results with the others shown in previous sections what are more representative since they were improved for giving the best flux. That is not the case in the next simulations, although they are completely acceptable to decide the best position of the chopper.

The results are plotted in Figure 16 and listed in Table 12.

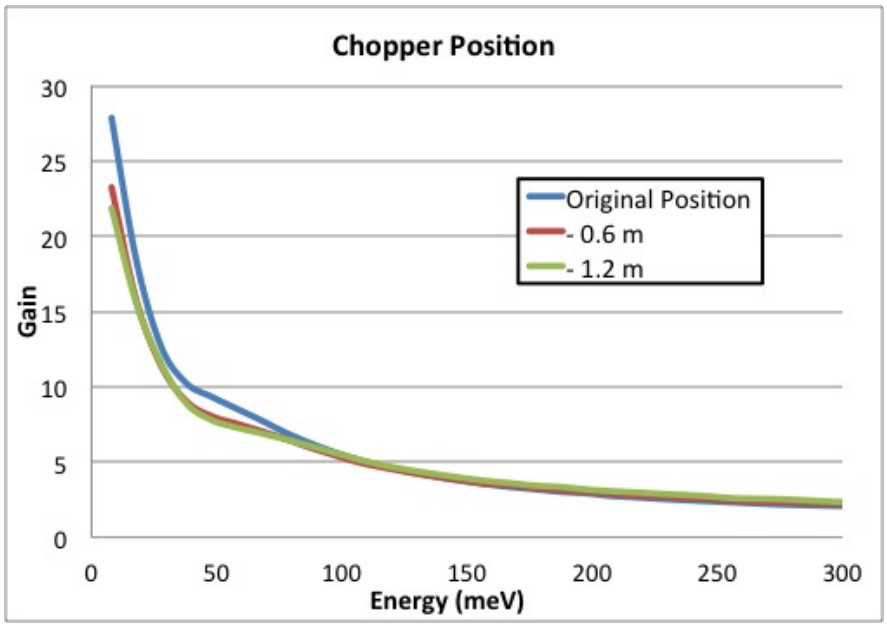

Figure 16: Chopper Position. Gain in Tapering Guide. In this simulation there is no guide in the shutter.

Energy at sample (meV)	Chopper Position		
	Original	- 0.6 m	- 1.2 m
10	27.8	23.2	21.9
20	18.4	15.7	15.5
50	9.4	8.1	7.8
100	5.6	5.4	5.6
150	3.8	3.8	3.9
200	2.9	3.0	3.2
250	2.4	2.5	2.7
300	2.1	2.2	2.3
350	1.9	2.0	2.2
400	1.8	1.9	2.0
566	1.5	1.6	1.7

Table 12: Chopper Position in Tapering Guide. Gain.

The slight differences observed after 100 meV can not determine which position for the chopper is the best in this range of energies, despite that the gains are greater at low energies when the chopper is placed at the original position. Intuitively, due to the tapering shape of the guide, if the gap, the chopper, is located closer to the moderator the cross section of this gap will be bigger that

implies larger loss of neutrons. Thanks to the small length of the chopper this loss is not too important at high energies, greater than 100 meV.

To prove this idea a total straight guide was simulated just changing the chopper position in the same way that has been done in the tapering guide. In a straight guide the cross section is conserved, because of that the loss of neutrons has to be independent of the chopper position. Figure 17 shows that.

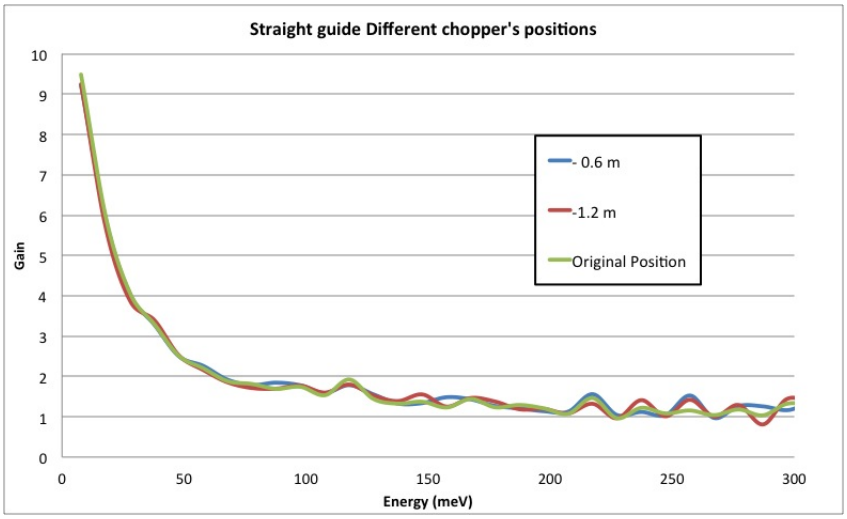

Figure 17: Chopper Position. Gain in Straight Guide.

Lines plotted are completely overlapped up to 100 meV. After that the results are too noisy for being analyzed correctly. Table 13 shows clearly the same conclusions.

Energy at sample (meV)	Chopper Position		
	Original	- 0.6 m	- 1.2 m
10	9.4	9.2	9.3
20	5.9	5.9	5.7
50	2.5	2.5	2.5
100	1.7	1.8	1.8
150	1.4	1.3	1.5
200	1.2	1.1	1.2
250	1.0	1.0	1.0
300	1.3	1.1	1.4
350	1.1	1.3	1.2
400	1.0	0.9	0.8
566	1.2	1.1	1.1

Table 13: Chopper Position. Gain in Straight Guide.

4.3 Snout

A novel component thought to be installed as an appendix to the conventional guide. This snout would be installed inside the instrument and not like a purely extension of the guide. It has 22 cm length and the exit of the snout is located 28 cm before the sample position.

Certain mobility is required by the instrument. For this reason the height of the snout is 5 mm greater in each cross directions, only in this case we can be sure that the adjust of the guide will remain satisfactory. The end of the guide has a cross section of 35 mm^2that is why the snout startswith a size of 40 mm, both in width and height.

The usefulness of installing this snout is analyzed in Figure 18.

The possibility of a change in the relative position of the snout relative to the fixed guide, if the instrument is required to be moved, has been studied conscientiously for understand how can affect the presence of the snout if a perfect alignment is not achieved.

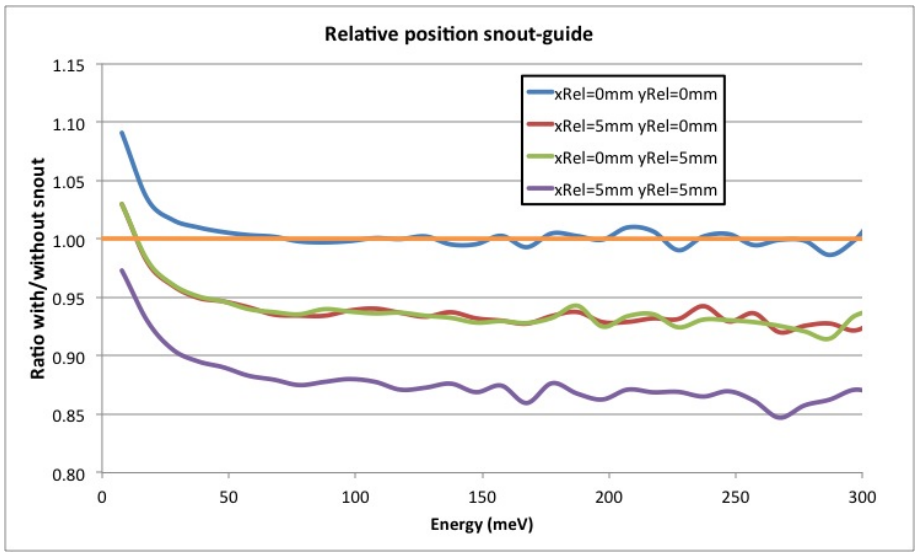

Figure 18: Gain using the snout. Positions are indicated relative to the perfectly centered snout position. Due to the symmetry of the guide theses positions can be understood as simetric distances long x and y directions. Is checked that a relative displacement in x edge provoked the same results as if it was in the y direction - green and red lines- .

The benefits of the snout are only obtained at very low energies and if and only if the snout is perfectly accurate in the center of the fixed guide. That encourage us to avoid the installation of the snout.

Despite this, the ideal case of the snout, that is, perfect centered relative position and a little bit tapered shape, from 40 mm at the beginning to 38 mm

at the exit, is compared with the guide without snout. Figure 19 and Table 14 detail the results.

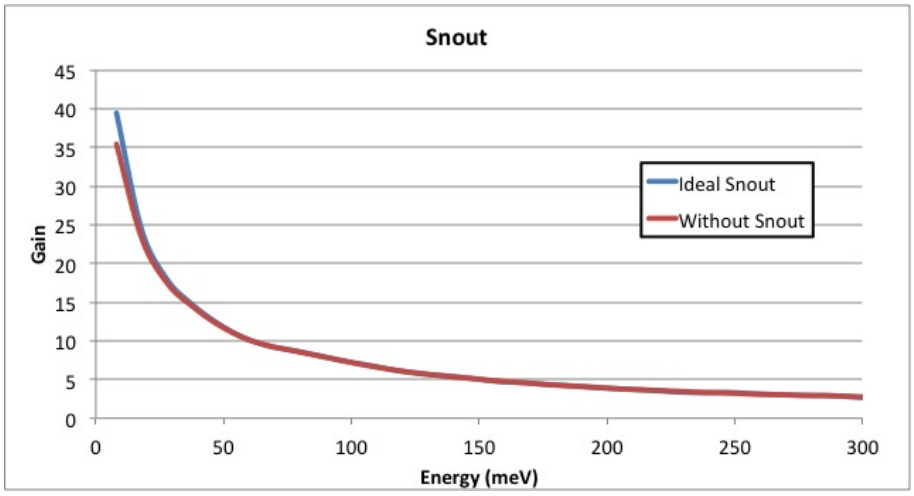

Figure 19: Gain in energy range 0-100 meV. Guide with Ideal snout against guide without snout.

Energy at sample (meV)	Ideal Snout	
	With	Without
10	39.5	35.4
20	24.3	23.3
50	12.2	12.1
100	7.4	7.4
150	5.1	5.1
200	3.9	4.0
250	3.3	3.3
300	2.7	2.8
350	2.5	2.5
400	2.4	2.2
566	1.9	1.9

Table 14: Guide with Ideal snout against guide without snout.

The best snout for TOSCA only can produces and increase in the gain at lowest energies. At energies greater than 20 meV the snout does not contribute for the flux.

The main reason is found at the end of the fixed guide. Here the guide presents a very focalized exit. Because of the gap existing until the snout the "focalized" neutrons produce a spray effect and, without snout, only achieve the

sample an amount equal that the snout can collect if we install it. If neutrons energy is really low the snout can collect these neutrons, which otherwise will be lost, but this energy range is negligible, 5 to 20 meV.

4.4 m-values optimization

Once the guide's geometry has been defined, is necessary to optimized the neutron flux at the sample with the minimum cost possible. Different simulations were considered, obtaining the results shown below. Comparisons made between all the possibilities allowed consider the best combination.

Modern neutron guide coating is composed of many layers of interspersed nickel and titanium, in order to achieve good reflectivity beyond the critical scattering vector. The performance of a guide coating is characterized by the reflectivity (the odds that an incoming neutron will be successfully reflected) as a function of the momentum transfer, Q [1].

The total price of the guide is determined by the m values chosen to cover the mirrors; see 4.4.1.

The selected distribution is detailed in Table 15.

McStas Name	AT (m)	l (m)	m
guide_shutter	1.625	1.938	3
guide_gap (*)	3.565	0.110	0
guide1_1	3.695	1.500	3
guide1_2	5.200	0.845	3
guide2_1	6.0405	1.5000	3
guide2_2	7.5410	1.4540	3
guide_vac_val	9.0270	0.0380	0
guide3	9.0655	0.3465	3
guide4 (Chopper)	9.4120	0.0870	0
guide5_1	9.5045	1.5000	4
guide5_2	11.0050	1.5000	4
guide5_3	12.5055	1.5000	5
guide5_4	14.0060	1.5000	5
guide5_5	15.5065	0.2585	6
guide6_1	15.7655	0.6000	6

Table 15: m values distribution.

Having compared many different distributions for m values, it was found

that the most sensitive section for changing the m reflective parameter is the one that is located after the chopper, so closer to the sample. It is consistent with the idea that the neutrons, because of the focusing behavior of the guide, need a better covered mirror where be reflected for remaining inside the guide.

The m values present in the legend adjacent to Figure 20 are the values after the chopper, while before it m=3 is chosen.

If the legend only displays one value for m this is aplied through all the guide after the chopper. If not, see Table 16 for further information.

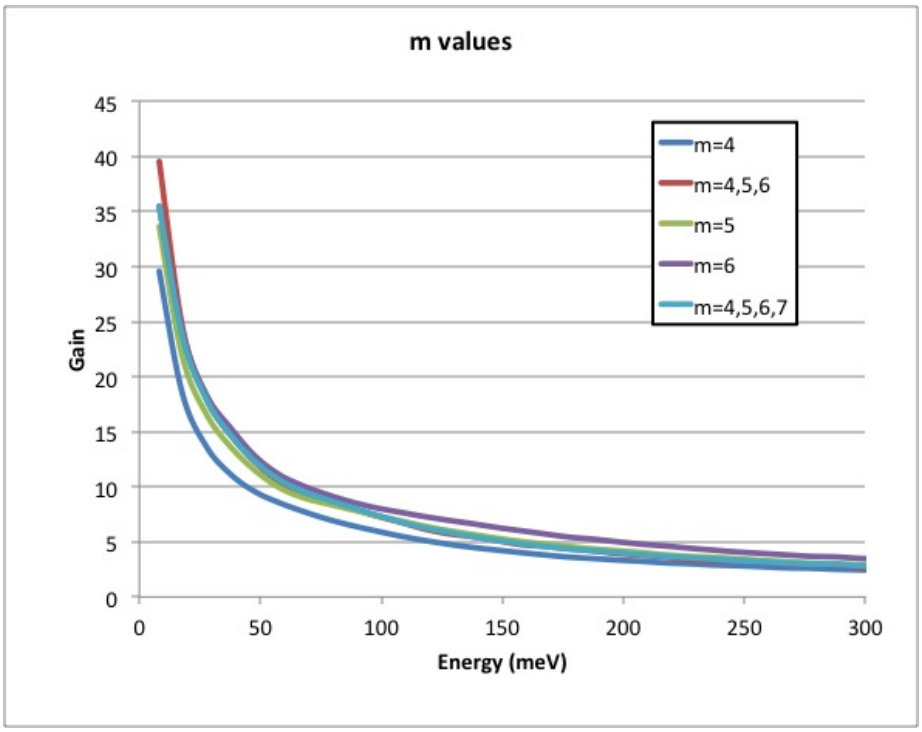

Figure 20: m values optimization.

The details for the m values distributed in the guide are:

Legend	guide5_1	guide5_2	guide5_3	guide5_4	guide5_5	guide6_1
m=4,5,6	4	4	5	5	6	6
m=4,5,6,7	4	4	5	5	6	7

Table 16: Legend table.

Distances of the guide components are detailed in Table 15 on the preceding page.

On Table 17 are listed the gain values for these simulations.

Energy at sample (meV)	m=4,5,6	m=4,5,6,7	m=4	m=5	m=6
10	39.5	39.7	29.6	33.6	39.8
20	24.3	24.6	18.3	21.7	24.9
50	12.2	12.3	9.5	11.5	12.8
100	7.4	7.5	6.0	7.4	8.1
150	5.1	5.2	4.3	5.3	6.3
200	3.9	4.0	3.3	4.2	5.0
250	3.3	3.3	2.8	3.5	4.1
300	2.7	2.8	2.5	2.9	3.5
350	2.5	2.6	2.2	2.6	3.1
400	2.4	2.3	2.0	2.4	2.7
566	1.9	1.9	1.7	1.9	2.2

Table 17: Gain for different m values distributions.

The differences between m=4,5,6 ; m=4,5,6,7 and m=5 are not too significant, so according to prices estimations presented in Subsection 4.4.1 the **most reasonable distribution seems m=4,5,6.**

The results for m=4 are, as expected, the worst, regarding flux at the sample, whereas the gain for m=6 is the best at all energies, however the huge cost of covering more than 6 m with m=6 is not set off by this gain.

4.4.1 Guide estimated price

The total guide price is defining by different parameters. Attending to the Reflectivity curve given by *SwissNeutronics:*

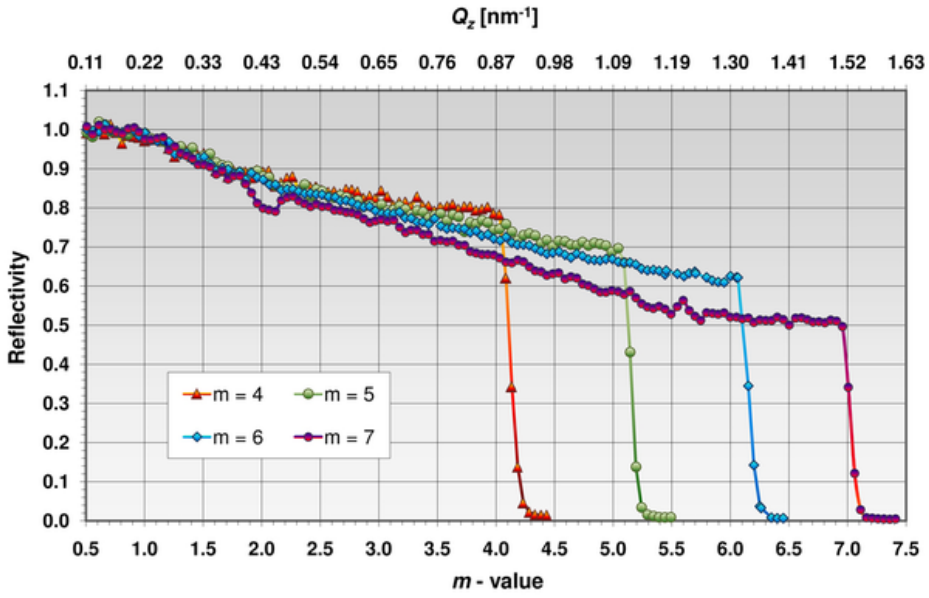

Figure 21: Guide reflectivity curve for m values.

Due the impossibility to have access to the current information about the costs of SwissNeutronics, the price was estimated, using the results presented by Kaspar Hewitt Kleno[1] in 2007.

$$price_1 = L \cdot PPM \tag{8}$$

where L is the total length of the guide and PPM is the price pr. meter of guide.

The price for a single vertical side (i.e. the left or right side) of a single guide section is given by:

$$price_2 = P_{m_i} \cdot l_i \cdot \frac{h_i + h_{i+1}}{2} \tag{9}$$

where P_{m_i} is the price pr. unit area of the coating value used for this section, l_i is its length and $\frac{h_i+h_{i+1}}{2}$ is its average height.

Following the same idea, the price for a single horizontal side (i.e. the top or bottom side) of a single guide section is given by:

$$price_3 = P_{m_i} \cdot l_i \cdot \frac{w_i + w_{i+1}}{2} \tag{10}$$

Additionally a price offset is used, signifying the price of the remainder of the instrument:

$$price_4 = P_{Off} \tag{11}$$

This is used to give a more realistic measure of cost efficiency, which will not diverge when using very cheap coating.

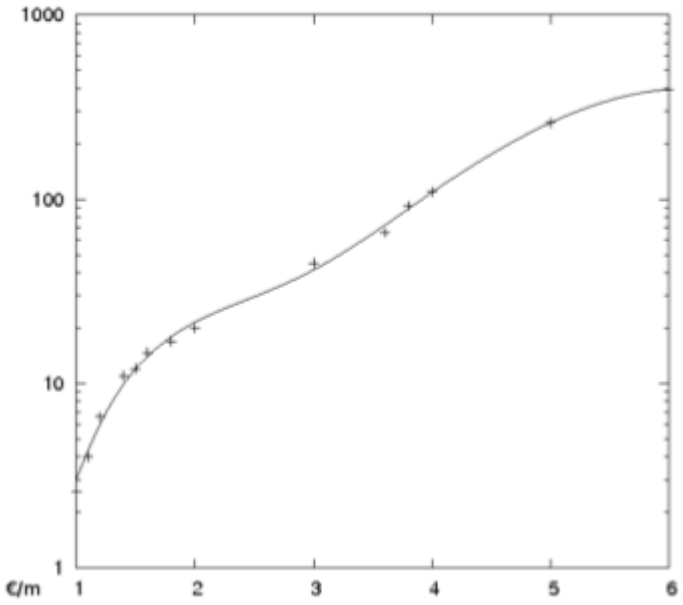

Figure 22: Logarithmic plot of coating price pr. unit area as a function of m-value, fitted to a 5th order polynomial. € in arbitrary units.

Putting the above together, we then have:

$$price_{total} = L \cdot PPM + P_{Off} + \sum i \left[P_{m_i} \cdot l_i \cdot \left(2 \cdot \frac{h_i + h_{i+1}}{2} + 2 \cdot \frac{w_i + w_{i+1}}{2} \right) \right] \tag{12}$$

where the sum is over the individual guide elements.

The values of P_{m_i} are based on data given by Peter Böni at SwissNeutronics in June 2007, and have been fitted to give the following 5th order polynomial, as a function of m, as shown in Figure 22:

$$P(m) = 54.1333 - 162.162 \cdot m + 173.312 \cdot m^2 - 76.366 \cdot m^3 + 15.1697 \cdot m^4 - 1.0404 \cdot m^5 \tag{13}$$

Note that the price given in equation 13 and Figure 22 has to be multiplied by a constant - which by request of SwissNeutronics is not published in this report - to give the absolute price.

Has been estimated the price of the guide relative for the price of a total covered m=3 guide. See Table 18.

Legend fig. 20	Price (Ratio with m=3)
m=4	1.6
m=4,5,6	2.3
m=5	2.8
m=6	3.9

Table 18: Price of the guide divided by the price of a guide with only m=3.

5 Conclusions

Simulations indicate that TOSCA will become in a global reference in spectroscopy research once the guide was installed. New doors of the subatomic world will be opened by the resolution what will be achieved with TOSCA.

The description of the guide is setting out in Table 19.

McStas Name	$\mathbf{w_1}$=$\mathbf{h_1}$ **(m)**	$\mathbf{w_2}$=$\mathbf{h_2}$ **(m)**	**AT (m)**	**l (m)**	m	Area/m^2
guide_shutter	0.100	0.100	1.625	1.938	3	0.7752
guide_gap (*)	0.100	0.100	3.565	0.110	0	—-
guide1_1	0.100	0.092	3.695	1.500	3	0.576
guide1_2	0.092	0.088	5.200	0.845	3	0.3042
guide2_1	0.088	0.080	6.0405	1.5000	3	0.504
guide2_2	0.080	0.073	7.5410	1.4540	3	0.445
guide_vac_val	0.073	0.073	9.0270	0.0380	0	—-
guide3	0.073	0.071	9.0655	0.3465	3	0.099
guide4 (Chopper)	0.071	0.071	9.4120	0.0870	0	—-
guide5_1	0.071	0.063	9.5045	1.5000	4	0.402
guide5_2	0.063	0.055	11.0050	1.5000	4	0.354
guide5_3	0.055	0.047	12.5055	1.5000	5	0.306
guide5_4	0.047	0.040	14.0060	1.5000	5	0.261
guide5_5	0.040	0.038	15.5065	0.2585	6	0.403
guide6_1	0.038	0.035	15.7655	0.6000	6	0.088

Table 19: TOSCA's guide setup.

The gain achieved with this guide, relative the current situation of TOSCA, without guide is plotted in Figure 20 and listed in Table 20.

5.1 Element description

Description of the individual elements in the TOSCA guide.

Shutter

McStas Name	$\mathbf{w_1}$=$\mathbf{h_1}$ **(m)**	$\mathbf{w_2}$=$\mathbf{h_2}$ **(m)**	**AT (m)**	**l (m)**	m	**slope (º)**
guide_shutter	0.10	0.10	1.625	1.938	3	0

Gap

McStas Name	$\mathbf{w_1}$=$\mathbf{h_1}$ **(m)**	$\mathbf{w_2}$=$\mathbf{h_2}$ **(m)**	**AT (m)**	**l (m)**	m	**slope (º)**
guide_gap (*)	0.10	0.10	3.565	0.110	0	0

$m = 0$: total absorbing area.

Insert (monolith)

McStas Name	w_1=h_1 (m)	w_2=h_2 (m)	AT (m)	l (m)	m	slope (^{o})
guide1_1	0.100	0.092	3.695	1.500	3	0.31
guide1_2	0.092	0.088	5.200	0.845	3	0.27

0.5 mm gap separating two parts of the insert guide.

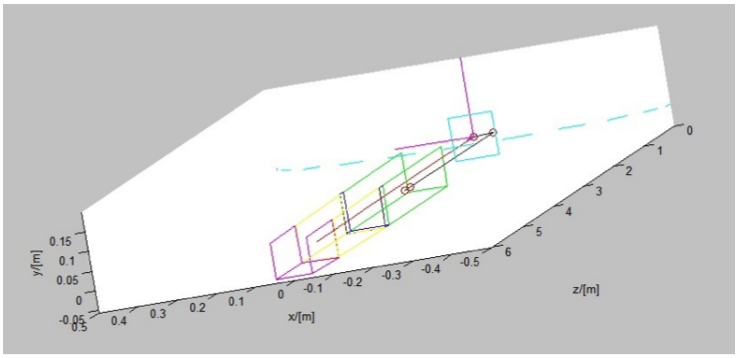

Figure 23: View of the guide components including, moderator (blue), shutter (green), insert in monolith (yellow and pink)

Guide before Vacuum Valve

McStas Name	w_1=h_1 (m)	w_2=h_2 (m)	AT (m)	l (m)	m	slope (^{o})
guide2_1	0.088	0.080	6.0450	1.500	3	0.31
guide2_2	0.080	0.073	7.5455	1.454	3	0.28

0.5 mm gap separating two parts of the guide before the vacuum valve.

Vacuum Valve

McStas Name	w_1=h_1 (m)	w_2=h_2 (m)	AT (m)	l (m)	m	slope (^{o})
guide_vac_val	0.073	0.073	9.027	0.038	0	0

Guide until chopper placement

McStas Name	w_1=h_1 (m)	w_2=h_2 (m)	AT (m)	l (m)	m	slope (^{o})
guide3	0.073	0.071	9.0655	0.3465	3	0.33

Chopper

McStas Name	w_1=h_1 (m)	w_2=h_2 (m)	AT (m)	l (m)	m	slope (^{o})
guide4 (Chopper)	0.071	0.071	9.4120	0.0870	0	0

Guide until monitors

McStas Name	w_1=h_1 (m)	w_2=h_2 (m)	AT (m)	l (m)	m	slope (º)
guide5_1	0.071	0.063	9.5045	1.5000	4	0.31
guide5_2	0.063	0.055	11.0050	1.5000	4	0.31
guide5_3	0.055	0.047	12.5055	1.5000	5	0.31
guide5_4	0.047	0.040	14.0060	1.5000	5	0.27
guide5_5	0.040	0.038	15.5065	0.2585	6	0.44

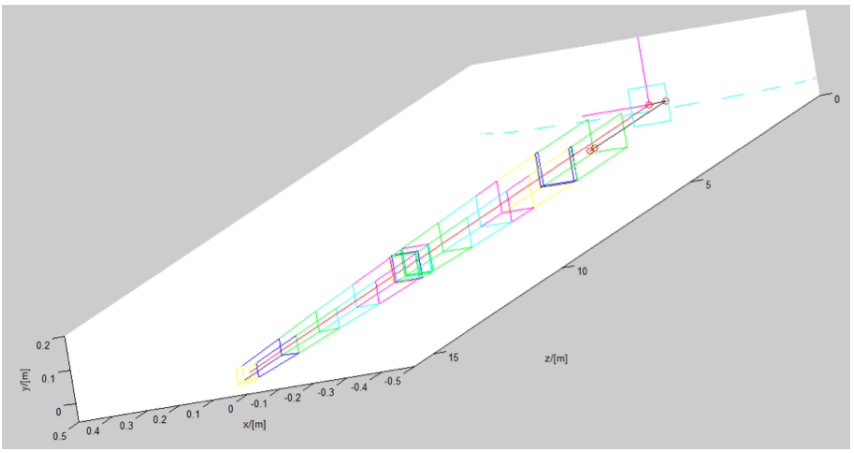

Guide after monitors

McStas Name	w_1=h_1 (m)	w_2=h_2 (m)	AT (m)	l (m)	m	slope (º)
guide6_1	0.038	0.035	15.7655	0.6000	6	0.29

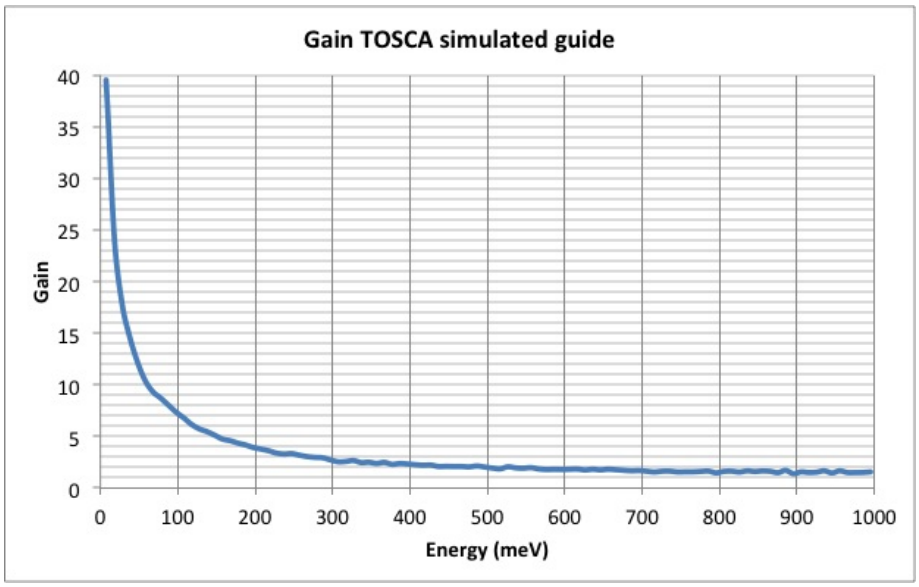

Figure 24: Gain achieved with TOSCA simulated guide between 0 and 1000 meV.

Energy at sample (meV)	Gain
10	39.5
20	24.3
50	12.2
100	7.4
150	5.1
200	3.9
250	3.3
300	2.7
350	2.5
400	2.4
566	1.9

Table 20: Gain achieved with TOSCA's guide.

The results obtained using the monitors placed at the sample position are:

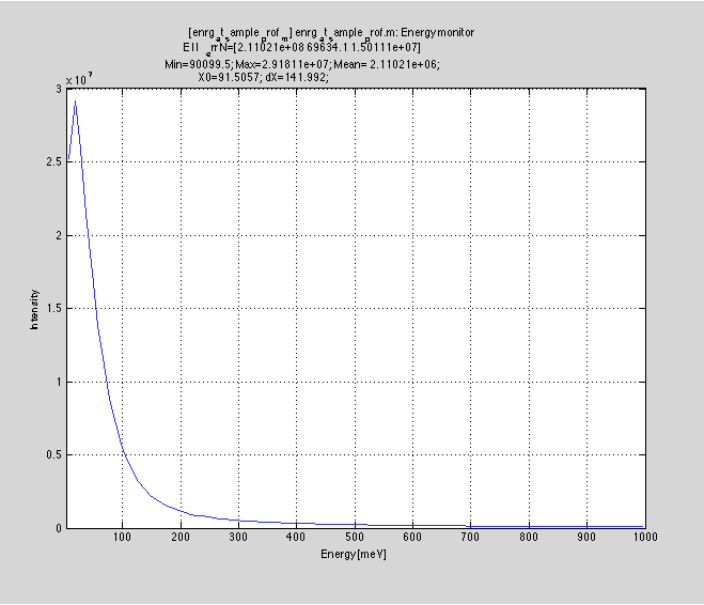

Figure 25: Intensity at sample against Energy 0-1000 meV

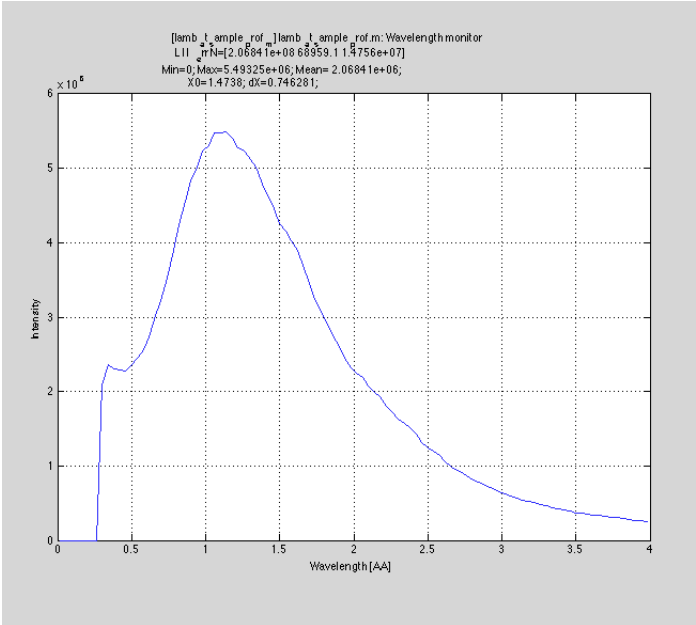

Figure 26: Intensity at sample against Wavelenght 0-4 Å

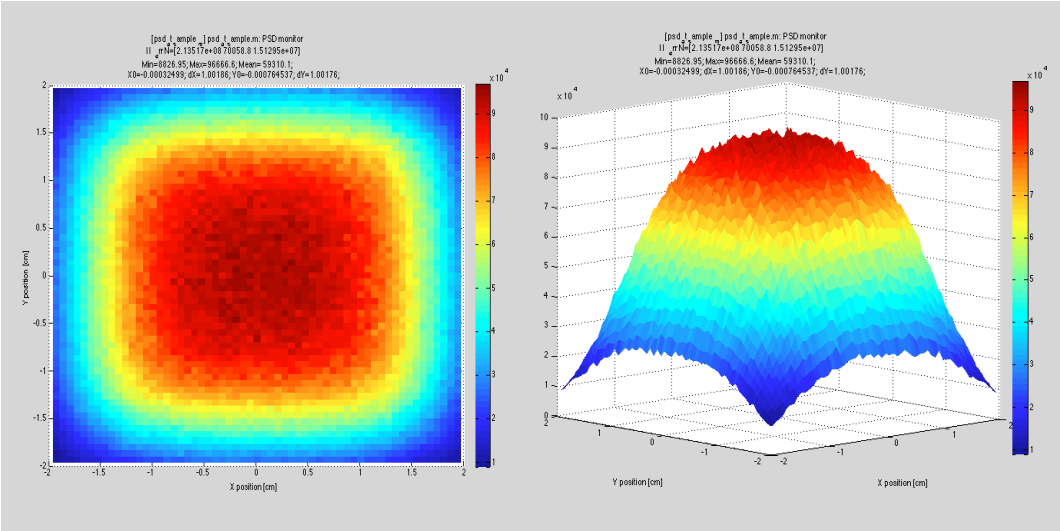

Figure 27: PSD monitor at sample.

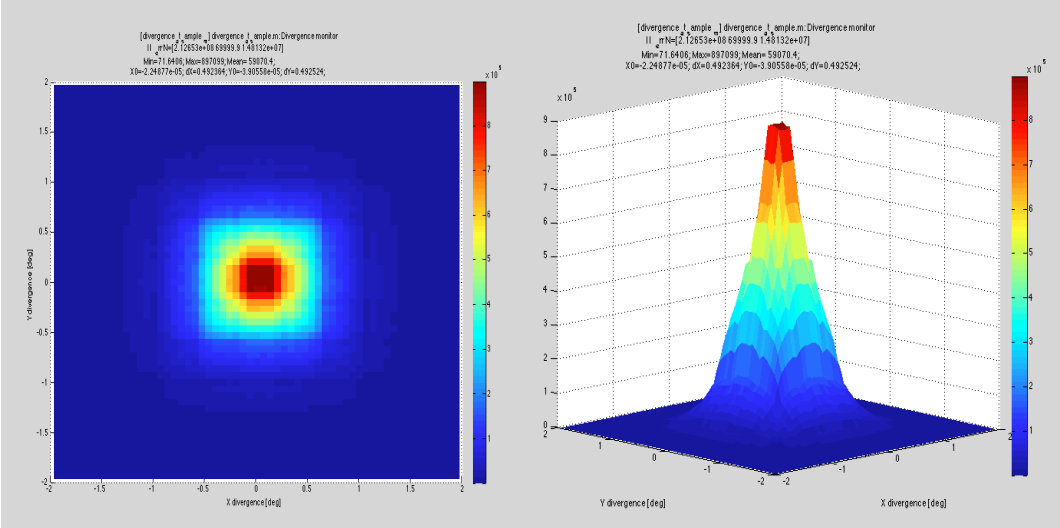

Figure 28: Divergence at sample.

6 Appendix

6.1 McStas code for TOSCA guide

/* Created by: Javier Fernández Castañón. ISIS - RAL */

DEFINE INSTRUMENT tosca(m_monolith,m_shutter, m_vac_val)

DECLARE
%{
double v_foc, c_h1,c_h2,slit_curv,num_slits,width_str; double lam,deg_phase,phase_time, phase;
double m_monolith, m_shutter, m_vac_val ;
%}

// #include <math.h>

INITIALIZE %{
%}

TRACE

COMPONENT Origin = Arm() AT (0,0,0) ABSOLUTE

COMPONENT source = ISIS_moderator(Face = "tosca", E0 = 1, E1 = 1000, dist = 1.625, xw = 0.11, yh = 0.11, modXsize = 0.11, modYsize = 0.11, CAngle = 0,SAC = 1) AT (0, 0, 0) RELATIVE Origin

COMPONENT guide_shutter = Guide_channeled(w1 =0.10, h1 =0.10, w2 =0.10, h2 = 0.10, l = 1.938, alphax = 4.38, alphay = 4.38 , W=3e-3, mx = m_shutter, my = m_shutter) AT (0, 0, 1.625) RELATIVE Origin

COMPONENT guide_gap = Guide_channeled(w1 =0.10, h1 =0.10, w2 =0.10, h2 = 0.10, l = 0.110, alphax = 4.38, alphay = 4.38 , W=3e-3, mx = 0, my = 0) AT (0, 0, 3.565) RELATIVE Origin

COMPONENT guide1_1 = Guide_channeled(w1 =0.10, h1 =0.10, w2 =0.09222, h2 = 0.09222, l = 1.5, alphax = 4.38, alphay = 4.38 , W=3e-3, mx = m_monolith, my = m_monolith) AT (0, 0, 3.695) RELATIVE Origin

COMPONENT guide1_2 = Guide_channeled(w1 =0.09222, h1 =0.09222, w2 =0.08783, h2 = 0.08783, l = 0.845, alphax = 4.38, alphay = 4.38 , W=3e-3, mx = m_monolith, my = m_monolith) AT (0, 0, 5.2) RELATIVE Origin

/*——————- Tapering guide m=3 ——————*/

COMPONENT guide2_1 = Guide_channeled(w1 =0.08783, h1 = 0.08783, w2 = 0.08 , h2 = 0.08 , l = 1.5, alphax = 4.38, alphay = 4.38 , W=3e-3, mx = 3, my = 3) AT (0, 0, 6.0455) RELATIVE Origin

COMPONENT guide2_2 = Guide_channeled(w1 =0.08, h1 = 0.08, w2 = 0.0725 , h2 = 0.0725 , l = 1.454, alphax = 4.38, alphay = 4.38 , W=3e-3, mx = 3, my = 3) AT (0, 0, 7.5460) RELATIVE Origin

/* ——————— monitors placed before vacuum valve ——————— */

COMPONENT lam_bef_vac_val = L_monitor(xmin=-0.04, xmax=0.04, ymin=-0.04, ymax=0.04, nchan=100, filename="lamb_bef_vac_val_prof", Lmin=0, Lmax=4) AT (0, 0, 8.9995) RELATIVE Origin

COMPONENT energy_bef_vac_val = E_monitor(xmin=-0.04, xmax=0.04, ymin=-0.04, ymax=0.04,Emin=3, Emax=1000, nchan=100, filename="enrg_bef_vac_val_prof") AT (0, 0, 8.9996) RELATIVE Origin

COMPONENT pixel_bef_vac_val = PSD_monitor(xmin=-0.04, xmax=0.04, ymin=-0.04, ymax=0.04, nx=60, ny=60, filename="psd_bef_vac_val") AT (0, 0, 8.9997) RELATIVE Origin

/*————————— Vacuum Valve 9027-9065 mm —————————*/

COMPONENT guide_vac_val = Guide_channeled(w1 =0.0725, h1 = 0.0725, w2 = 0.0725 , h2 = 0.0725, l = 0.038, alphax = 4.38, alphay = 4.38 , W=3e-3, mx = m_vac_val, my = m_vac_val) AT (0, 0, 9.027) RELATIVE Origin

/* ————————— Guide until CHOPPER —————————*/

COMPONENT guide3 = Guide_channeled(w1 = 0.0725, h1 = 0.0725 , w2 = 0.0707, h2 = 0.0707, l = 0.3465, alphax = 4.38, alphay = 4.38 , W=3e-3, mx = 3, my = 3) AT (0, 0, 9.0655) RELATIVE Origin

/* ————————— monitors placed before chopper ————————— */

COMPONENT lam_bef_chop = L_monitor(xmin=-0.04, xmax=0.04, ymin=-0.04, ymax=0.04, nchan=100, filename="lamb_bef_chop_prof", Lmin=0, Lmax=4) AT (0, 0, 9.4116) RELATIVE Origin

COMPONENT energy_bef_chop = E_monitor(xmin=-0.04, xmax=0.04, ymin=-0.04, ymax=0.04,Emin=3, Emax=1000, nchan=100, filename="enrg_bef_chop_prof") AT (0, 0, 9.4117) RELATIVE Origin

COMPONENT pixel_bef_chop = PSD_monitor(xmin=-0.04, xmax=0.04, ymin=-0.04, ymax=0.04, nx=60, ny=60, filename="psd_bef_chop") AT (0, 0, 9.4118) RELATIVE Origin

/* ————————— CHOPPER 9412 - 9499mm —————————-*/

COMPONENT guide4 = Guide_channeled(w1 = 0.0707, h1 = 0.0707, w2 = 0.0707, h2 =0.0707 , l = 0.087 , alphax = 4.38, alphay = 4.38 , W=3e-3, mx = 0, my = 0) AT (0, 0, 9.4120) RELATIVE Origin

/* ————————— monitors placed after chopper ————————*/

COMPONENT lam_after_samp = L_monitor(xmin=-0.04, xmax=0.04, ymin=-0.04, ymax=0.04, nchan=100, filename="lamb_aft_chop_prof", Lmin=0, Lmax=4) AT (0, 0, 9.5000) RELATIVE Origin

COMPONENT energy_after_samp = E_monitor(xmin=-0.04, xmax=0.04, ymin=-0.04, ymax=0.04,Emin=3, Emax=1000, nchan=100, filename="enrg_aft_chop_prof") AT (0, 0, 9.5020) RELATIVE Origin

COMPONENT pixel_after_samp = PSD_monitor(xmin=-0.04, xmax=0.04, ymin=-0.04, ymax=0.04, nx=60, ny=60, filename="psd_aft_chop") AT (0, 0, 9.5040) RELATIVE Origin

/*————————— Tapering guide after chopper —————————*/

COMPONENT guide5_1 = Guide_channeled(w1 = 0.0707 , h1 = 0.0707 , w2 = 0.0629 , h2 = 0.0629 , l = 1.5 , alphax = 4.38, alphay = 4.38 , W=3e-3, mx = 4, my = 4) AT (0, 0, 9.5045) RELATIVE Origin

COMPONENT guide5_2 = Guide_channeled(w1 = 0.0629 , h1 = 0.0629 , w2 = 0.05513 , h2 = 0.05513 , l = 1.5 , alphax = 4.38, alphay = 4.38 , W=3e-3, mx = 4, my = 4) AT (0, 0, 11.0050) RELATIVE Origin

COMPONENT guide5_3 = Guide_channeled(w1 = 0.05513 , h1 = 0.05513 , w2 = 0.04735 , h2 = 0.04735 , l = 1.5 , alphax = 4.38, alphay = 4.38 , W=3e-3, mx = 5, my = 5) AT (0, 0, 12.5055) RELATIVE Origin

COMPONENT guide5_4 = Guide_channeled(w1 = 0.04735 , h1 = 0.04735 , w2 = 0.03956 , h2 = 0.03956 , l = 1.5 , alphax = 4.38, alphay = 4.38 , W=3e-3, mx = 5, my = 5) AT (0, 0, 14.006) RELATIVE Origin

COMPONENT guide5_5 = Guide_channeled(w1 = 0.03956 , h1 = 0.03956 , w2 = 0.03822 , h2 = 0.03822 , l = 0.2585 , alphax = 4.38, alphay = 4.38 , W=3e-3, mx = 6, my = 6) AT (0, 0, 15.5065) RELATIVE Origin

/* ———— Extend the guide until the sample ————-*/

COMPONENT guide6_1 = Guide_channeled(w1 = 0.03822 , h1 = 0.03822 , w2 = 0.035 , h2 = 0.035 , l = 0.620 , alphax = 4.38, alphay = 4.38 , W=3e-3, mx = 6 , my = 6) AT (0, 0, 15.7655) RELATIVE Origin

/* NO SNOUT */

/* —— sample 40x40 mm and guide apperture 35x35 mm —— */

COMPONENT lam_at_samp = L_monitor(xmin=-0.02, xmax=0.02, ymin=-0.02, ymax=0.02, nchan=100, filename="lamb_at_sample_prof", Lmin=0, Lmax=4) AT (0, 0, 17.0) RELATIVE Origin

COMPONENT energy_at_samp = E_monitor(xmin=-0.02, xmax=0.02, ymin=-0.02, ymax=0.02,Emin=3, Emax=1000, nchan=100, filename="enrg_at_sample_prof") AT (0, 0, 17.001) RELATIVE Origin

COMPONENT pixel_at_samp = PSD_monitor(xmin=-0.02, xmax=0.02, ymin=-0.02, ymax=0.02, nx=60, ny=60, filename="psd_at_sample") AT (0, 0, 17.002) RELATIVE Origin

COMPONENT diverg_at_samp = Divergence_monitor(nh=60, nv=60, filename="divergence_at_sample", xmin=-0.02, xmax=0.02, ymin=-0.02, ymax=0.02 ,h_maxdiv=2, v_maxdiv=2) AT (0, 0, 17.003) RELATIVE Origin

END

6.2 ISIS-TS1-BEAMLINE N8 - TOSCA

Instrument Technical Specification (Version 1)

Item of Equipment	Existing Instrument	Upgraded Instrument
Moderator Type h2o (upper)	Viewable face 100 x100mm Umbra size 85x85mm Can thk 3mm Al	(size TBE) Can thk 3mm Al
Void Vessel Windows(#1&2)	2 X 0.5mm Al.	2 x 0.5mm Al.
Collimation Ray Layout	Drg SI-2541-309	???????
Shutter Collimation Window #3	(b4c Collimation Assy. 0R2541-046) 1 x window 0.5 mm thk. Input (mm) 84.5/84.0 w x 80.6/80.0 h- 1605mm from mod cl. Exit(mm)73.5/73.0 w x 74.5/74.0 h- 3565mm from mod cl.	 Window #3 Glass Guide
Window #4	1 x window 0.5 mm thk.	Window #4
Insert Collimation Assembly Window #5	(b4c Collimation) SI-2541-400 1x window 0.5mm thk Input collimation 75.1 mm SQ. 3695mm from mod cl. Exit collimation 69 mm SQ. (5977mm from mod) End of tube 6040 from mod cl.	 Window #5 Glass guide
Secondary Collimation Assembly	(b4c Collimation) SI-2541-430	
Secondary collimation Tube 1	(B4c) OR-2541-067 Ff 6097.5 from mod cl Rf 8529.5 from mod cl	Stain S. Bellows Glass guide in Stain S. Vac box
Secondary collimation Tube 2	(B4c) SI-2541-439 Ff 8529.5 from mod cl Rf 8994.5 from mod cl	Glass guide in Stain S. Vac box
Monitor	None	New Scintillator or Bead Monitor Mounted in plane of chopper cut (Requires circular cut out through guide wall)
Gate Valve	VAT Valve DN100 Series 08	VAT Valve DN100 Series 08
Gate Valve Window #6	SI-2541-398 0.5mm thk Al	Gate Valve Window #6
Bellows	None	Stain S. Bellows
Glass guide in vac box	None	Glass guide in vac box
Chopper Window #7	0.5 thk Al. Alloy	Window #7- 0.5 thk Al. Alloy
T-Zero Chopper	0-SI-2700-001 (Nimonic Design) Modified Internally with 4 bladed 15mm thk cadmium disc Designed for 60x60mm Beam Centre=9479mm from mod	Double Disk CR Chopper Similar to SI-8827-001 Nimonic Chopper not required
Chopper Window #8	0.5 thk Al. Alloy	Window #8- 0.5 thk Al. Alloy (Vanadium foil if using Bead Monitor!)
Glass guide in vac box	None	Glass guide in vac box
Monitor	None	New Scintillator or Bead Monitor Mounted in plane of chopper cut (Requires circular cut out through guide wall)
Window #9	SI-2541-440 0.5mm thk Al.	none
Secondary collimation Tube 3	SI-2541-438 – 1720 lg.	Glass Guide in vac box

	Ff 9879mm from mod cl Rf 11599mm from mod cl	
Secondary collimation Tube 4	SI-2541-438-1720 lg Ff 11604mm from mod cl Rf 13324mm from mod cl	Glass Guide in vac box
Secondary collimation Tube 5	OR-2541-067-2432 lg. Ff 13329mm from mod cl Rf 15761mm from mod cl	Glass Guide in vac box
Window #10	3-SI-2541-440 0.5mm thk Al.	Window #9
Monitor	Beam Monitor	Beam Monitor or New Scintillator Monitor
TFXA Detector Box Assembly	SI-2541-134	
Window #11	Window SI-2541-171 0.24mm THK	Window #10
Vacuum Vessel (Tube)	SI-2541-170 (385mm lg)	Glass Guide in Vac box
Bellows Assy	SI-2541-173 (80 mm lg Noml)	Bellows Assy
Vacuum Vessel (Tube)	SI-2541-174 (325mm lg)	Glass Guide snout inside vacuum vessel tube
Sample Position	17m from Mod Size 40 x 40mm	17m from Mod Size 35 x 35mm
T2 SAMPLE AREA	DRG SI-2541-490	

6.3 Legend. McStas Parameters listed

Parameters presented during the report and in McStas code are detailed, in alphabetical order, in Table 21.

Parameter	**Description**
alphax	(Å) Slope of reflectivity for left and right vertical mirrors in each channel
alphay	(Å) Slope of reflectivity for top and bottom mirrors
AT (m)	(m) Distance from the center of moderator
CAngle	(radians) Angle from the centre line
dist	(m) Distance from source to the focusing rectangle
Emax	(meV) Maximum energy to detect
Emin	(meV) Minimum energy to detect
E0	(meV) Lower edge of energy distribution
E1	(meV) Upper edge of energy distribution
filename	Name of file in which to store the detector image (text)
h_maxdiv	(degrees) Maximal horizontal divergence detected
h_1	(m) Height at the guide entry
h_2	(m) Height at the guide exit
l	(m) Length of guide
Lmax	(Å) Upper edge of wavelength distribution
Lmin	(Å) Lower edge of wavelength distribution
m_monolith	m parameter in monolith guide. *m = 3 (user input)*
m_shutter	m parameter in shutter guide. *m = 3 (user input)*
m_vac_val	m parameter in vacuum valve guide. *m = 0 (user input)*
modXsize	(m) Moderator vertical size
modYsize	(m) Moderator horizontal size
mx	m-value of material for left and right vertical mirrors in each channel. Zero means completely absorbing
my	m-value of material for top and bottom mirrors. Zero means completely absorbing
nchan	(1) Number of wavelength/energy channels
nh	(1) Number of pixels columns
nv	(1) Number of pixels rows
nx	(1) Number of pixel columns
ny	(1) Number of pixel rows
SAC	(boolean) Apply solid angle correction or not (1/0)
target_index	(1) relative index of component to focus at, e.g. next is +1 this is used to compute 'dist' automatically.
v_maxdiv	(degrees) Maximal vertical divergence detected
w_1 (m)	(m) Width at the guide entry
w_2 (m)	(m) Width at the guide exit

Parameter	**Description**
W	($Å^{-1}$) Width of super-mirror cut-off for all mirrors
xmax	(m) Upper x bound of detector opening
xmin	(m) Lower x bound of detector opening
xw	(m) Width of focusing rectangle
ymax	(m) Upper y bound of detector opening
ymin	(m) Lower y bound of detector opening
yw	(m) Height of focusing rectangle

Table 21: Description parameters TOSCA guide.

References

[1] K. H. Kleno, "Simulating neutron guides for simulating neutron guides for the european spallation source," tech. rep., Niels Bohr Institute - University of Copenhagen, October 2008.

[2] P. Mitchell, *Vibrational spectroscopy with neutrons: with applications in chemistry, biology, materials science and catalysis*, vol. 3. World Scientific Pub Co Inc, 2005.

[3] J. T. Timmy Ramirez-Cuesta, Stewart Parker, *TOSCA User Manual*. RAL - ISIS, STFC, Harwell Oxford, Didcot, OX11 0QX, United Kingdom.

[4] S. Yang, J. Sun, A. J. Ramirez-Cuesta, S. K. Callear, W. I. F. David, D. Anderson, R. Newby, A. Blake, J. Parker, C. Tang, and M. Schröder, "Selectivity and direct visualisation of carbon dioxide and sulphur dioxide in a decorated porous host," *Nature Chemistry*, no. in press, 2012.

[5] E. F. Peter Willendrup, Erik Knudsen and K. Lefmann, *User and Programmers Guide to the Neutron Ray-Tracing Package McStas*. RISØ DTU, Risø DTU, Roskilde, Denmark, version 1.12 ed., May 2011.

[6] K. H. Klenø, K. Lefmann, P. Willendrup, P. Böni, and E. Farhi, "Powerful and cost-effective elliptical neutron guide designs for the ess,"

[7] I. Anderson, L. Radcliffe, J. Haines, and K. Crawford, "Conceptual design document for the sing (sns instruments - next generation) project," Tech. Rep. SNS SINGPRJ-10-PN0002-R01, OAK Ridge National Laboratory, U.S. Department of Energy, Oak Ridge, Tennessee 37831-6285, March 2004.

[8] R. Reidel, "Spallation neutron source," Tech. Rep. IS-1.7.3.2-4034-SP-A-00.

[9] D. Abernathy, "Spallation neutron source," Tech. Rep. IS-1.18.4-6033-RE-A-00.

[10] H. Häse, A. Knöpfler, K. Fiederer, U. Schmidt, D. Dubbers, and W. Kaiser, "A long ballistic supermirror guide for cold neutrons at ill," *Nuclear Instruments and Methods in Physics Research Section A: Accelerators, Spectrometers, Detectors and Associated Equipment*, vol. 485, no. 3, pp. 453–457, 2002.

[11] H. Abele, D. Dubbers, H. Häse, M. Klein, A. Knöpfler, M. Kreuz, T. Lauer, B. Märkisch, D. Mund, V. Nesvizhevsky, *et al.*, "Characterization of a ballistic supermirror neutron guide," *Nuclear Instruments and Methods in Physics Research Section A: Accelerators, Spectrometers, Detectors and Associated Equipment*, vol. 562, no. 1, pp. 407–417, 2006.